

DELIVERABLE

D26.8 Testing and verification of the European Seismic Risk Model (ESRM20)

Work package	WP26 (JRA4: Risk Modelling Framework for Europe)
Lead	EUCENTRE
Authors	<p>Helen Crowley, EUCENTRE Jamal Dabbeek, EUCENTRE Florencia Victoria De Maio (EUCENTRE) Venetia Despotaki (formerly GEM Foundation / EUCENTRE) Daniela Rodrigues (formerly EUCENTRE) Marta Faravelli, EUCENTRE Barbara Borzi, EUCENTRE Vitor Silva, GEM Foundation Luis Martins, GEM Foundation Petros Kalakonas, GEM Foundation Graeme Weatherill, GFZ Potsdam Evi Riga, AUTH Anna Karatzetzou, AUTH Kyriazis Pitilakis, AUTH Anastasios Anastasiadis, AUTH Dimitrios Pitilakis, AUTH Stavroula Fotopoulou, AUTH Alberto Michellini, INGV Licia Faenza, INGV</p>
Reviewers	Management Board
Approval	Management Board
Status	Final
Dissemination level	Public
Delivery deadline	30.04.2020
Submission date	28.04.2020
Intranet path	DOCUMENTS/DELIVERABLES/SERA_D26.8_testing_verification_ESRM20.pdf



Table of Contents

Summary	3
1 Introduction	4
2 Unit Tests	5
2.1 Exposure Model.....	5
2.2 Vulnerability Model.....	7
3 Integration Tests.....	12
3.1 Hazard Curves and Vulnerability Models	12
3.2 Ground Motion, Vulnerability and Exposure Models.....	12
3.3 Vulnerability and Exposure Models.....	13
3.3.1 Europe.....	13
3.3.2 Italy	14
3.3.3 Greece.....	16
4 System Tests	21
4.1 Resolution of Exposure Models	21
4.2 Disaggregation of the Exposure Model	23
4.3 Testing Exposure Model Resolution	26
4.3.1 National level.....	26
4.3.2 Sub-national level.....	29
4.4 Remarks on the Exposure Resolution.....	30
5 Acceptance Testing	32
5.1 National Risk Assessments	32
5.2 Global Earthquake Model	33
5.3 Global Assessment Report (GAR).....	34
6 Concluding Remarks.....	36
7 References	37
Contact	40

Summary

This deliverable describes the testing framework that is being set up for the testing of the European Seismic Risk Model 2020 (ESRM20) model before its official release later this year. This framework leverages software development and includes unit tests, integration tests, system tests and acceptance tests. Unit tests consider the components of the risk model separately, whereas integration tests check the performance of a group of components together. Example integration tests include history checks where the total losses (fatalities and economic losses) estimated from all events in the European earthquake catalogue since 1980 will be undertaken, and comparisons will be made with the total observed losses and empirically derived annual average losses and loss exceedance curves (with the losses adjusted to today's value). To constrain the ground motion in the previous test, ShakeMaps for the historical events over the aforementioned period are being used to predict the damage / losses / consequences using the 'Scenario from ShakeMap' calculator of the OpenQuake-engine and these are being compared with the reported numbers in loss databases. More detailed verification tests are also being made for events in Italy and Greece for which detailed damage data at the building-by-building level is available. In order to test the resolution of the European risk model, system tests which check the impact of different levels of resolution on the resulting AAL and loss exceedance curves is also being undertaken. Finally, acceptance tests are based on comparing the losses with other similar models and sharing the results with the main stakeholders of the model.

1 Introduction

Following the developments of SERA WP26 (JRA4), a European seismic risk model will be released in 2020, once the European seismic hazard model from WP25 (JRA3) is finalised. The main risk metrics that will be released with the model include national and sub-national maps of average annual loss (AAL) and probable maximum loss (PML) and national loss exceedance curves for 45 countries in Europe. Before the release of this model, the performance of its components needs to be extensively evaluated through a number of different tests.

Taking inspiration from the four levels of software testing (see e.g. <https://www.seguetech.com/the-four-levels-of-software-testing/>), the tests of the European Seismic Risk Model (ESRM20) have been divided into the following four categories: unit tests, integration tests, system tests, and acceptance tests.

- Unit testing: during this first round of testing, a computer program is typically submitted to assessments that focus on specific units or components of the software to determine whether each one is fully functional. For ESRM20 a unit test might, for example, look separately at the performance of the fragility, vulnerability or exposure components. Unit tests are presented in Chapter 2.
- Integration testing: in this level of testing a number of units within a program are combined and tested as a group. Within ESRM20, an example of an integration test combining the exposure and vulnerability would be to estimate the losses from past events using ShakeMaps (with well constrained ground motions) to compare the estimated and observed losses. Integration tests are presented in Chapter 3.
- System testing: this is the first level in which the complete application is tested as a whole. Within ESRM20, all of the outputs of the model (i.e. average annual losses at national and sub-national levels for residential, commercial and industrial occupancy types and national loss exceedance curves) will need to be calculated at a resolution that leads to reliable results within reasonable run-times. System tests are provided in Chapter 4.
- Acceptance testing: the final level of testing is conducted to determine whether the system is ready for release. A workshop to investigate a wide range of results of the ESRM20 with an audience of experienced risk modellers (some of whom will also be end-users/stakeholders) is planned before the release of the model. Comparisons of the results will also be made against other initiatives that have covered European risk such as the Global Assessment Report (GAR, 2015), GEM's Global Risk Map v2018.1 (Silva et al., 2020) as well as national risk assessments and insurance/reinsurance industry models (where available). Acceptance testing is presented in Chapter 5.

This deliverable outlines the testing framework of the European Seismic Risk Model (ESRM20) and presents a number of illustrative examples of the tests. It is noted that some of these tests have been undertaken using the source model from the previous European hazard model (ESHM13; Woessner et al., 2013) and they will thus need to be repeated once the European Seismic Hazard Model (ESHM20) is finalised.

2 Unit Tests

For ESRM20, the unit tests that have been planned consider separately the performance of the exposure, fragility, and vulnerability components, as described in the following sections.

2.1 Exposure Model

The development of the exposure models relies on a number of different sources of data and expert judgment that are integrated to produce a final model (see SERA Deliverable D26.3; Crowley et al., 2020). A number of tests of the final model are needed to ‘sanity check’ the integration of these different sources. A number of exposure metrics are automatically extracted from each country-based exposure model, such as the average population per dwelling, average dwelling area, area of dwellings per capita, the average number of dwellings per building, the average dwelling cost, and ratios of the total replacement cost between commercial and residential, industrial and residential and commercial and residential buildings. It is expected, for example, that the residential building stock should have a higher total value than the commercial building stock which in turn should be higher than the industrial building stock. Some exposure metrics can be checked against census data (such as that which was collected as part of the NERA project¹, see Figure 1) and outliers can be easily identified and, where necessary, corrected. Other sources that can be used to verify the exposure model include the residential, industrial and commercial capital stock values in the GAR (GAR, 2015) model (see Figure 2), as well as data on the GDP per sector for industry and services that can be found in online sources such as those provided by the World Bank or the national statistics office of each country (see Figure 3 and Figure 4).

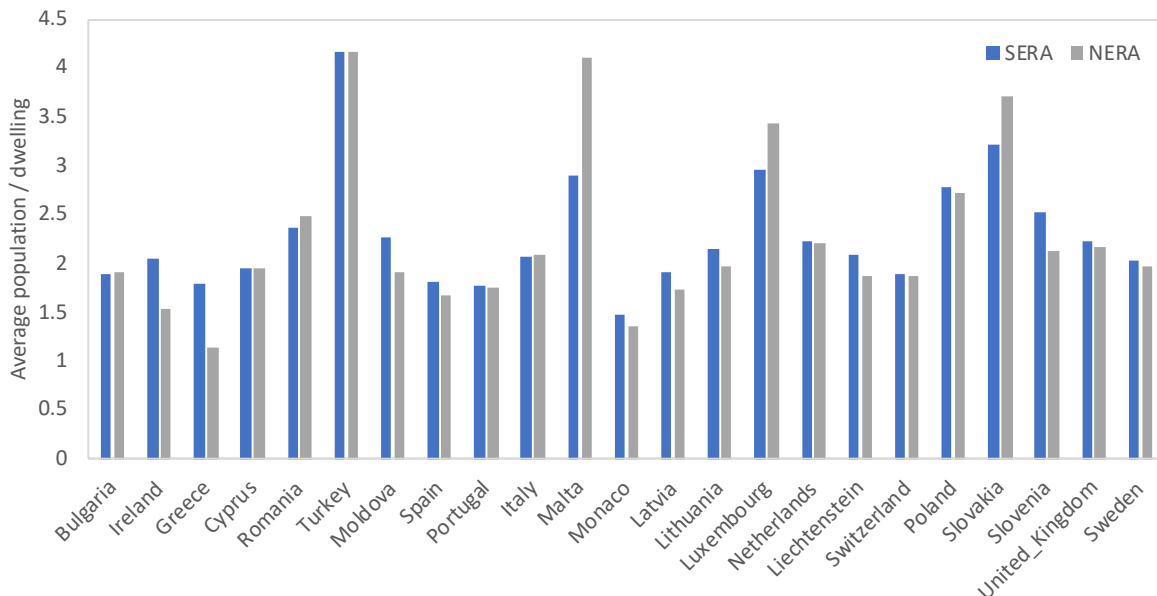


Figure 1. Comparison of the average population per dwelling in the latest SERA exposure model against data collected in the NERA project

¹ https://gitlab.seismo.ethz.ch/efehr/esrm20_exposure/-/blob/master/res_mapping_schemes/NERA_Level0_v3.0.xlsx

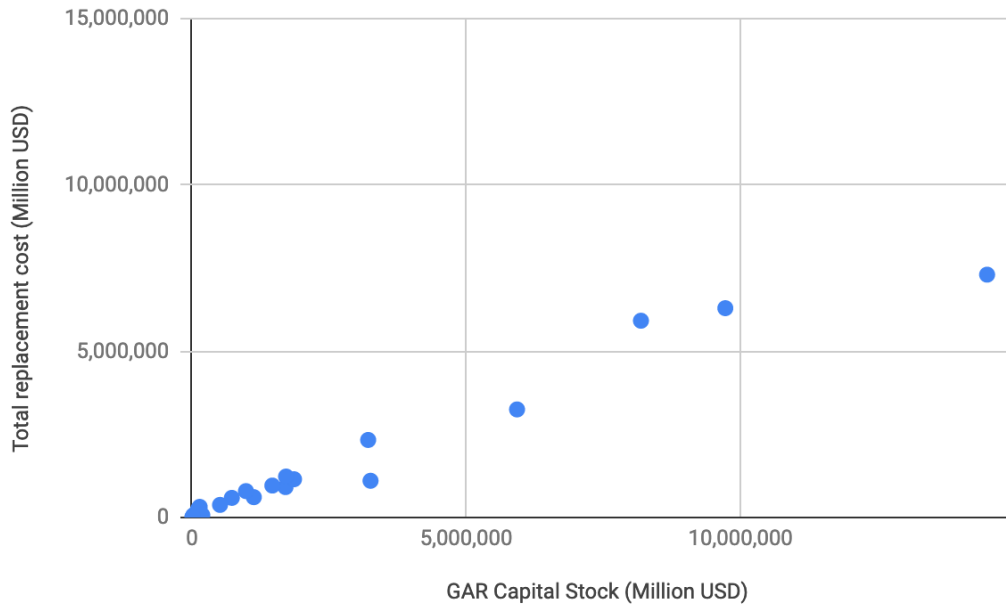


Figure 2. Comparison of proportion of GAR Capital Stock (in million USD) in the services sector for each European country compared to the total replacement cost in the current version of the ESRM20 model

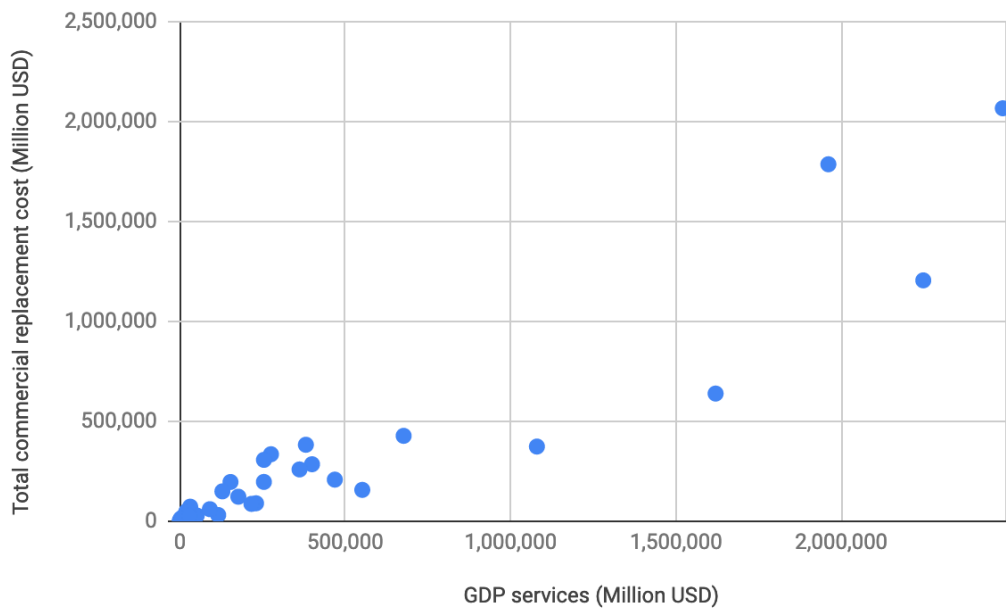


Figure 3. Comparison of proportion of GDP (in million USD) in the services sector for each European country compared to the total commercial replacement cost in the current version of the ESRM20 model

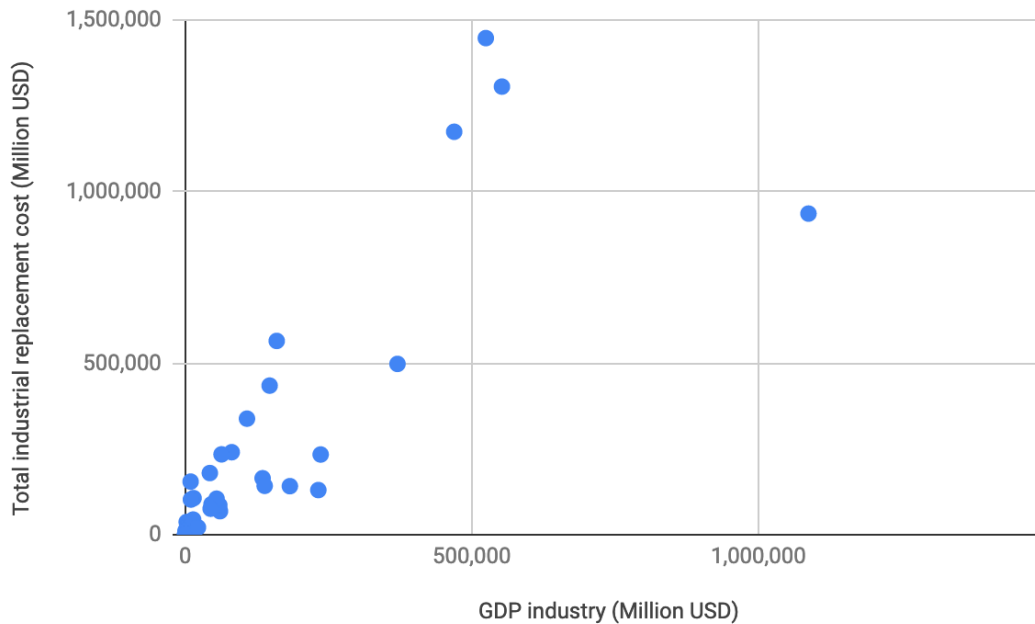


Figure 4. Comparison of proportion of GDP (in million USD) in the services sector for each European country compared to the total industrial replacement cost in the current version of the ESRM20 model

Figure 2 shows a good correlation between the total replacement cost and the GAR (2015) Capital Stock, with lower values for the former which is expected as it includes structures and machinery that is not included in the residential, commercial and industrial building categories of the ESRM20. Figure 3 and Figure 4 shows good correlation between the services and industry GDP and the commercial and industrial replacement cost, respectively. Nevertheless, this ongoing evaluation of the exposure model has highlighted some outliers in terms of countries with higher industrial than commercial replacement costs which will need to be investigated and possibly corrected before the final model can be released and used in the risk calculations.

2.2 Vulnerability Model

A number of unit tests of the vulnerability models are undertaken, starting with the fragility functions that are used to develop the vulnerability models. A few minor checks are first performed:

- A check is made that the dispersion of the lognormal fragility functions is between 0.3 and 0.8. Values less than 0.3 are low given all of the uncertainties in the framework (see SERA Deliverable D26.5) and values above 0.8 mean that the intensity measure is not efficient and should be checked.
- The median values of the lognormal fragility functions for slight damage and complete damage are checked. Based on engineering judgment, the median value for slight damage should be greater than 0.1g when the intensity measure is PGA (which corresponds to an AvgSa of around 0.16g²) and complete damage median values should be less than 2g PGA (corresponding to an AvgSa of around 3g).

² The intensity measure being investigated for use in the risk model is AvgSa (currently defined as the geometric mean of the spectral ordinates for the following periods of vibration: T=[0.0756, 0.1302, 0.1848, 0.2394, 0.294, 0.3486, 0.4032, 0.4578, 0.5124, 0.567]). It has been found that the average ratio of PGA to AvgSa for the records being used in the fragility function development is around 0.64.

- A check is made that none of the damage state fragility functions cross (i.e. the probability of exceeding a given damage state should be higher than the probability of exceeding the subsequent (higher) damage state).

Following these checks, a relative comparison of the fragility between different construction materials and lateral load resisting systems is made to check whether they match engineering judgment and observations from past European earthquakes. It is noted that because AvgSa is a sufficient intensity measure (see e.g. Bianchini et al., 2009) it can be used for many building classes, thus allowing direct comparisons of the fragility of these classes. Figure 5 presents a comparison of various subsets of the reinforced concrete classes in order to check whether the influence of design code, lateral force coefficient, number of storeys and lateral load resisting system on the relative fragility is as expected.

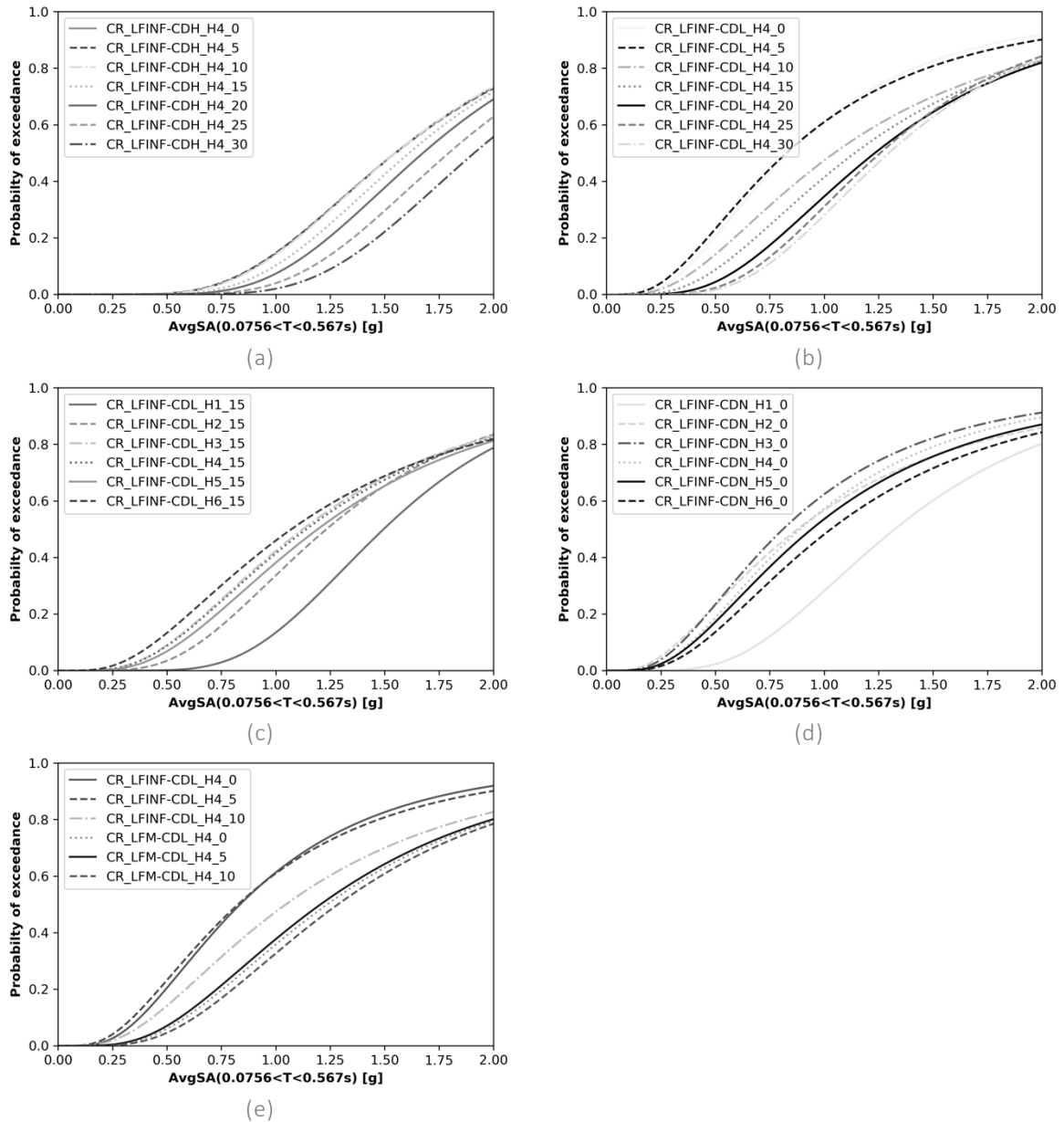


Figure 5. Comparison of the reinforced concrete (CR) complete damage fragility functions for (a) 4 storey (H4) infilled frames (LFINF) with high code design (CDH) in terms of lateral force coefficient, (b) 4 storey infilled frames with low code design (CDL) in terms of lateral force coefficient, (c) infilled frames with low code design and 15% lateral force coefficient in terms of number of storeys, (d) infilled frames with no seismic design (CDN) in terms of number of storeys, (e) 4 storey low code design in terms of infilled versus bare frames (LFM)

Indeed, Figure 5a and Figure 5b show that higher lateral forces in the design lead to lower levels of fragility and the lower design code level leads to higher fragility. A low number of storeys is seen to lead to lower fragility in Figure 5c and Figure 5d, and the moment frame fragility functions of Figure 5e are less fragile than the infilled framed functions. Figure 6a presents a comparison of the complete damage unreinforced masonry fragility functions developed for European buildings, and it shows that the trend of fragility is as expected – the most fragile type of construction is adobe, and the least fragile is the concrete block unreinforced masonry. Figure 6b shows a comparison of different material and lateral load resisting system types, where the least fragile is the steel braced frame and the most fragile is unreinforced masonry.

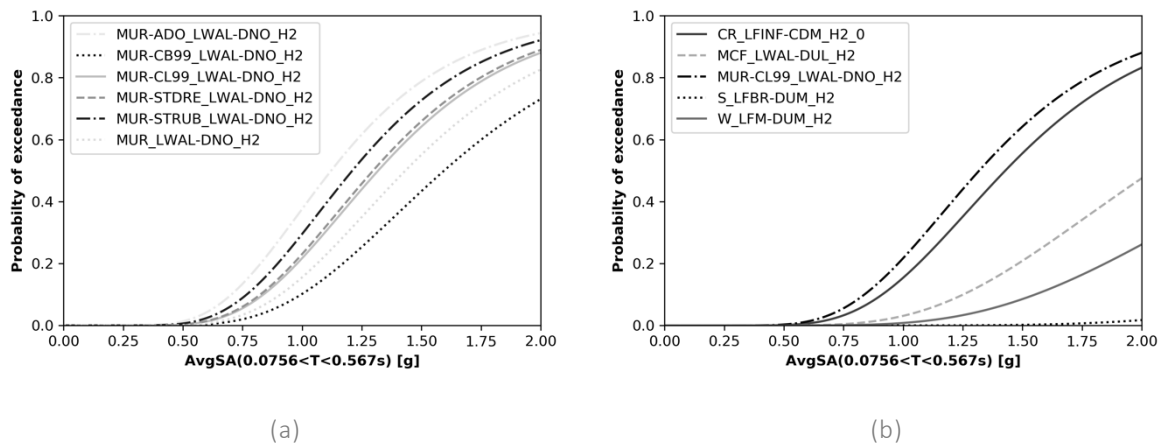


Figure 6. Example of the comparison of the complete damage fragility functions for different types of (a) 2 storey European unreinforced masonry buildings, (b) 2 storey European building classes with different material and lateral load resisting material types

A comparison with a selection of the existing fragility and vulnerability functions that have been collected as part of the SERA project (see Deliverable D25.5 and the associated database³) is being carried out to ensure that the proposed models are in line with previous studies performed in Europe. For comparison with other models it is necessary to use alternative intensity measures as other studies have not used the same definition of AvgSa that has been used herein. Figure 7 shows a comparison of some of the classes of reinforced concrete frames with functions from the literature. In terms of PGA (g).

In Figure 7a, b and c the models developed within the SERA project (based on the methodology in Deliverable D26.5 and referred to as ‘Romão et al. 2019’) are seen to compare well with the Borzi et al. (2008a) functions (for 4 storeys) which are based on a similar analytical model, whereas the 2 and 3 storey Del Gaudio et al. (2019) functions are less fragile, which is due to a stronger influence of the number of storeys in this study, which was based on empirical damage data from the Da.D.O database (Dolce et al., 2019). Moment frames (without infills) are compared in Figure 7b, c and d and, as expected, the Borzi et al. (2007, 2008a and 2008b) models are similar to the Romão et al. (2019) functions. Such comparisons will continue to be undertaken for the other building classes in the model to check whether there are any functions which differ greatly from previous research.

³ https://gitlab.seismo.ethz.ch/efehr/esrm20_vulnerability

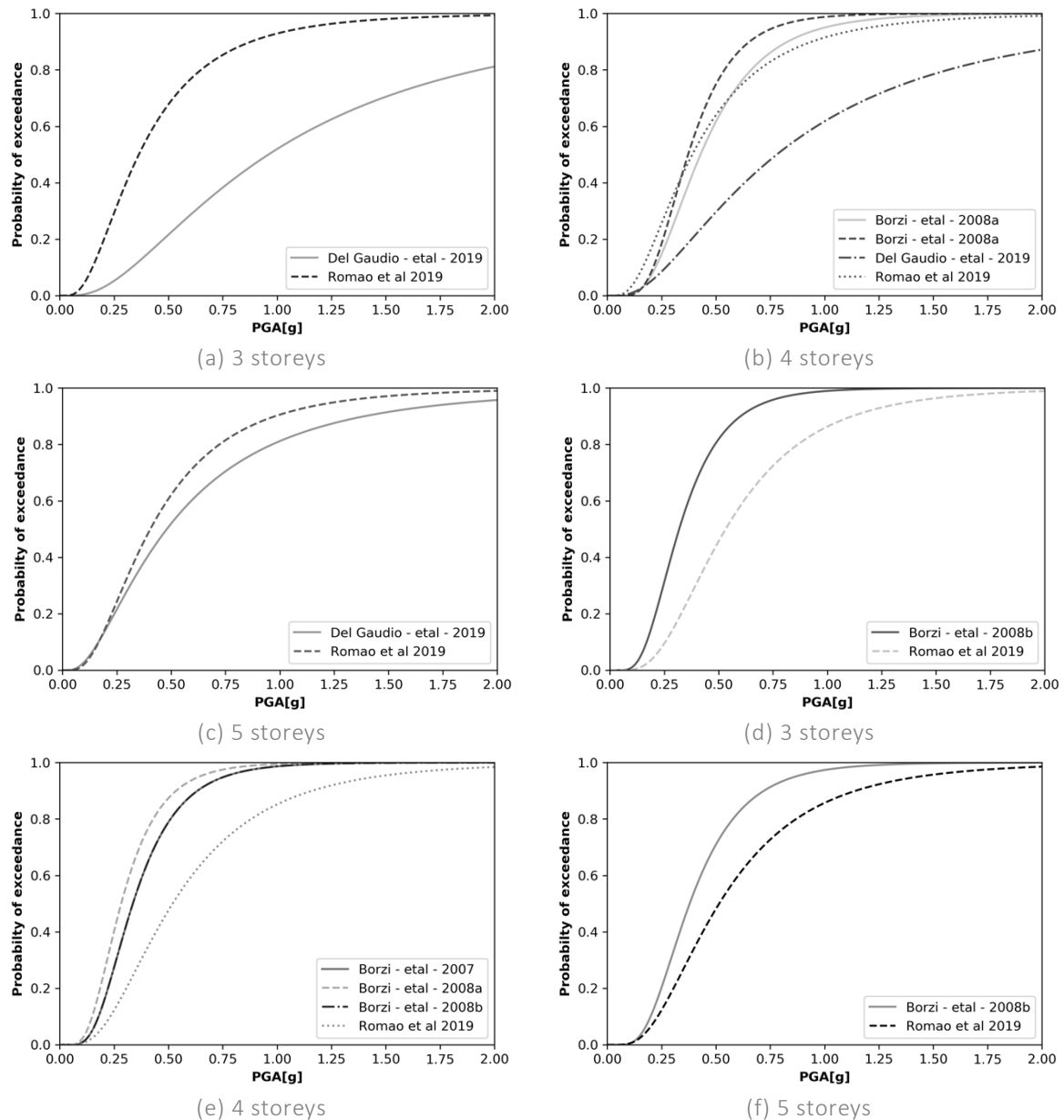


Figure 7. Comparison of the complete damage European reinforced concrete fragility functions (Romão et al., 2019) with functions from the literature (a to c) 3, 4 and 5 storey infilled reinforced concrete frames with no seismic design, (d to e) 3, 4 and 5 storey moment frames with no seismic design

It should be considered when undertaking the comparisons shown above that many of the models in the academic literature have not been calibrated or tested using past earthquake damage and loss data. Hence, although comparisons with existing models is an important unit test, it is even more important to ensure that the proposed models are tested against empirical data. In order to compare the proposed vulnerability models for economic loss and fatalities for a given country with empirically derived models, a mean vulnerability function calculated through an exposure-weighted combination of all the building classes in the country is being undertaken. These vulnerability functions (in terms of both economic loss and fatalities) can then be compared with the empirical models developed by PAGER (Jaiswal et al., 2009; Jaiswal and Wald, 2013). The latter models are in terms of MMI and so, for comparison purposes, all analytical models have been estimated in terms of spectral acceleration at 0.3 s and converted to macroseismic intensity. The Faenza and Michelini (2010) ground motion intensity conversion equation (GMICE) has been used and the mean and mean ± 1 standard deviation intensities have been computed. Figure 8 shows comparisons of the European weighted analytical vulnerability

models in terms of both economic loss and fatalities with PAGER’s empirical models for both Italy and Greece.

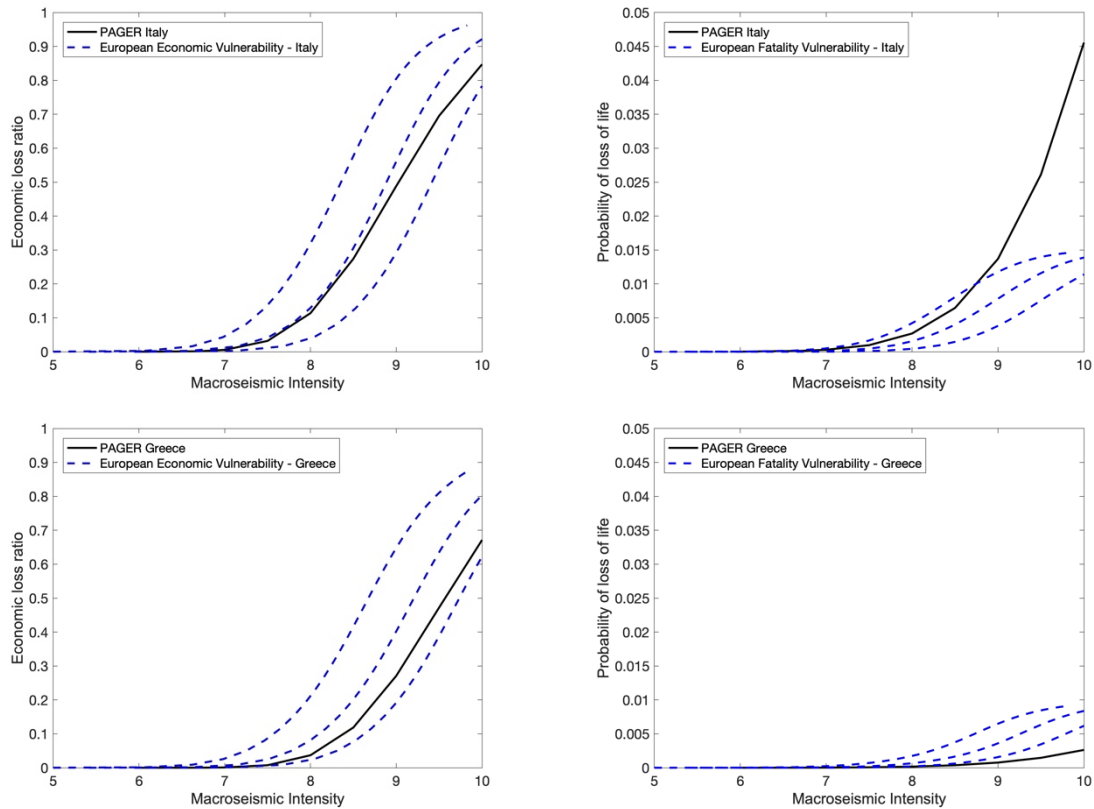


Figure 8. Comparison of the PAGER country-based economic (left) and fatality (right) vulnerability models with the current analytical European vulnerability models for Italy (top) and Greece (bottom). The three dotted lines show the functions with the mean and ± 1 standard deviation of the ground motion intensity conversion equation.

This figure shows that for Italy the economic vulnerability models compare well with the empirical PAGER models, whereas the fatality models lead to lower estimations than PAGER. Similar findings for the economic loss have been found for Greece, whereas a slight overestimation of past fatalities has instead been observed. This test demonstrates that more focus needs to be placed on the European fatality model before proceeding to system and acceptance testing. However, to avoid differences caused by the fatality data availability between countries, a mean function for Europe will also be produced and compared with a mean function from all European countries available in PAGER.

3 Integration Tests

In this level of testing a number of components of ESRM20 are combined and tested as a group.

3.1 Hazard Curves and Vulnerability Models

The average annual collapse probability and average annualized loss ratios (AALR) for a number of cities in Europe with different levels of hazard are also being computed. These are integration tests as they combine the hazard and vulnerability components of the risk model. Currently hazard curves have been computed using the ESHM13 source zone model with the ESRM20 ground motion and site model, but these will be replaced with the full ESHM20 curves once they become available. This test can be used to identify excessively vulnerable (or excessively resistant) building classes. For example, the average annual collapse probability should fall between 10^{-3} and 10^{-6} . As an example of the AALR test, the comparison between the AALRs aggregated by macro-building classes (i.e. CR/LDUAL, CR/LFINF, CR/LFM, CR/LWAL, MCF, MR, MUR, S/LFBR, S/LFINF, S/LFM, S/LWAL and W – see legend for definition) is provided in Figure 9, for 5 locations in Europe with different levels of hazard (Vienna, Lisbon, Rome, Athens and Istanbul).

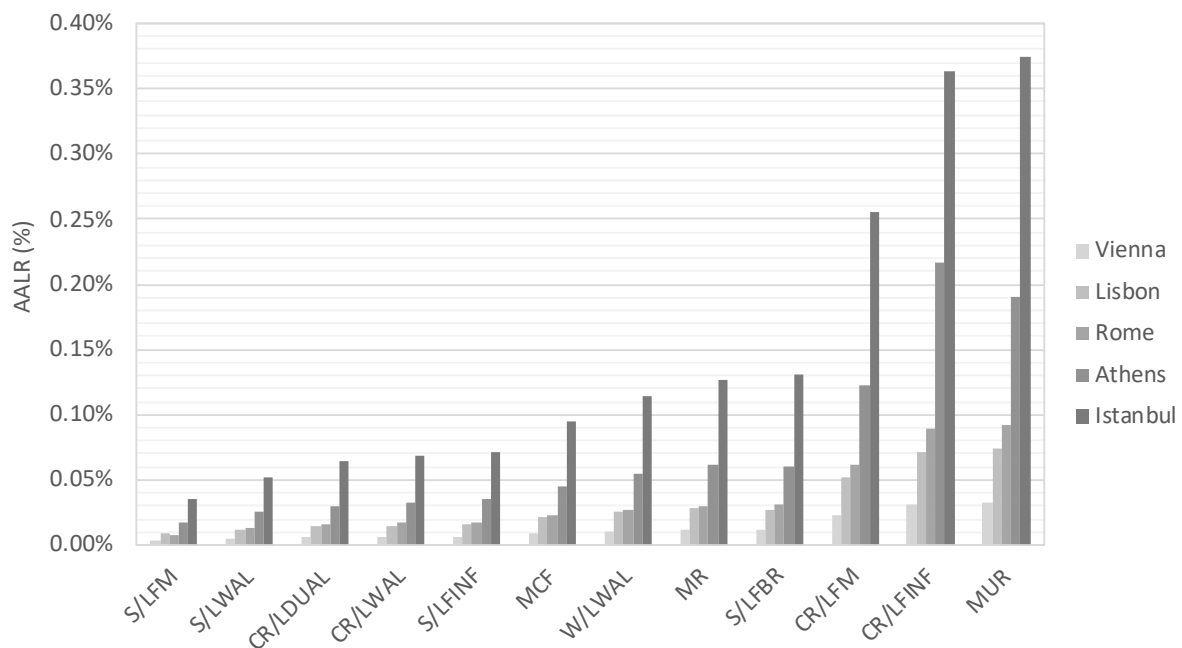


Figure 9. Comparison of AALR for different two-storey macro building classes in five cities in Europe: Note, S: Steel, W: Wood, MUR: unreinforced masonry, MR: reinforced masonry, MCF: confined masonry, CR: reinforced concrete, LFM: moment frame, LWAL: bearing wall, LDUAL: dual wall-frame system, LFINF: infilled frame.

3.2 Ground Motion, Vulnerability and Exposure Models

Another integration test is planned to test the ground motion, exposure and vulnerability together through a 'history check'. The total losses (fatalities and economic losses) estimated from all events in the EMEC earthquake catalogue since 1980 will be undertaken by randomly simulating ground motion fields using the latest European ground motion logic tree, and combining them with the European exposure and vulnerability models to estimate economic losses and fatalities. These results can then

be compared with the total observed losses and empirically derived annual average losses and loss exceedance curves (with the losses adjusted to today's value). Sources of loss data for this purpose include NatCatService database (Munich Re, 2019) for economic loss and Centre for Research on the Epidemiology of Disasters (CRED)'s EMDAT database (EMDAT, 2019). It is important to note when carrying out these comparisons is that these disaster databases cover the entire built environment which include infrastructure impacts (and not just the residential, commercial and industrial buildings that are considered here).

3.3 Vulnerability and Exposure Models

In order to focus the integration tests on the vulnerability and exposure models, constrained ground motions from ShakeMaps or physics-based modelling of the ground motion from past events can also be undertaken. These tests might look at the statistics for a number of events (as in the test above) or a more detailed test for a single event can be performed.

3.3.1 Europe

The current European vulnerability and exposure models have been tested using damage and loss data from European past events between 1980 and 2017 from the NatCatService database (Munich Re, 2019). In this process, USGS ShakeMaps were used with the European exposure dataset and the fragility and vulnerability functions in order to estimate the number of collapsed buildings and direct economic losses, respectively. The framework employed for these calculations is described in Silva and Horspool (2019) and has been implemented in the OpenQuake-engine as the 'Scenario from ShakeMap' calculator. A number of randomly generated ground motion fields (considering spatial and inter-period correlation of the spectral ordinates) have been generated from the median and uncertainty ShakeMaps and then these have been combined with the exposure and vulnerability to estimate the mean loss. A comparison between the estimated and observed losses (adjusted to 2017 values) is depicted in Figure 10.

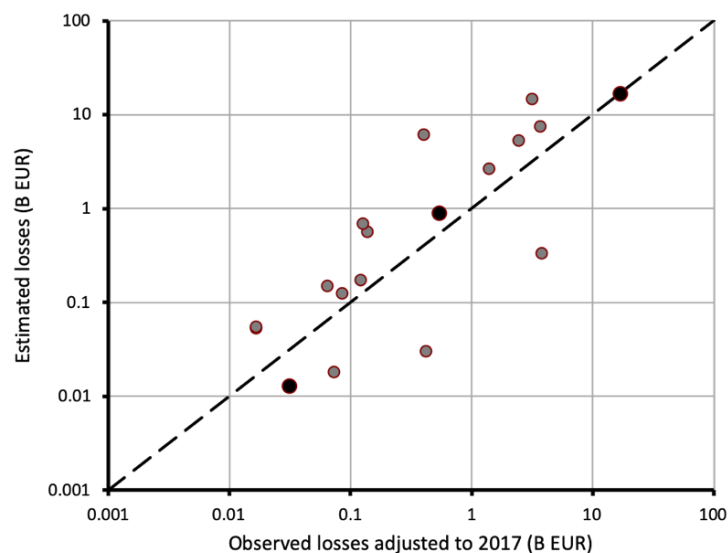


Figure 10. Comparison between estimated and observed losses for over 20 past events in Europe using USGS ShakeMaps

Although a fair agreement between the estimated and observed losses was obtained (with limited bias), there is clearly a large dispersion in the results. Reasons for this variability include differences in the

exposure model and the actual built environment, bias in the collection of the observed damage and losses, and large uncertainty in the ground shaking due to lack of recording stations in the affected regions (e.g. Villar-Vega and Silva, 2017). In order to reduce these uncertainties, more detailed focus on specific events has also been undertaken, as described in the following sections.

3.3.2 Italy

In Italy it has been possible to compare the estimation of damage using the European fragility functions with observed damage using the damage data for individual buildings that is available in the Da.D.O database (Dolce et al., 2019).

Through collaboration with JRA6 (Real Time Earthquake Shaking), ShakeMaps for the following historical sequences of events in Italy have been calculated: Irpinia 1980, Umbria-Marche 1997, Pollino 1998, Molise 2002, L'Aquila 2009 and Emilia 2012. The ShakeMap v4 system (<https://github.com/usgs/shakemap>) has been used to calculate median and uncertainty ShakeMaps for each earthquake associated with each sequence of events with magnitude greater than Mw 5. The following intensity measures have been considered: MCS, PGA, PGV, SA(0.3), SA(1.0). An ensemble ShakeMap for each sequence has then been calculated by taking the maximum value of each intensity measure at each location. The locations in the ShakeMaps are associated with the location of the buildings included in the Da.D.O database.

The damage data in the Da.D.O. database has required additional processing before being used to test the analytical fragility functions as it does not include all of the undamaged buildings (except for the Irpinia event which included all buildings in the region). The ISTAT census data from 1991, 2001 and 2011 has been used to estimate the total number of reinforced concrete and masonry buildings in each municipality and then the number of damaged buildings from Da.D.O. has been removed to estimate the number of undamaged buildings. So far, only those municipalities where the inspection forms made up at least 80% of the number of buildings in the municipality have been considered in the calculations herein (as it cannot necessarily be assumed that municipalities with few damage forms had few damaged buildings). The data is thus biased to damaged municipalities, and thus the tests can only provide insight into how well the fragility functions predict damage rather than how well they predict the lack of damage.

Exposure models for each event were thus developed using the data from Da.D.O. and appropriate analytical fragility functions from the European model (Deliverable D26.5) were mapped to the building classes. The same calculation framework described in Section 3.3.1 for Europe has been used to test the fragility functions. The results for all sequences are presented in Figure 11 where it can be seen that very good comparisons are available for L'Aquila 2009 and Emilia 2012, whereas an underestimation of the damage is obtained for the other events.

The significant damage is well estimated for Irpinia 1980, but there is an underestimation of the lower damage states. For Molise, Pollino and Umbria, a clear underestimation of all damage states is seen. Although an attempt to account for the sequence of ground shaking has been made by taking into account the maximum level of ground shaking for each event in the sequence, the possibility that accumulation of damage from each event could have influenced the fragility of the buildings has not been considered and this might explain the underestimation of damage. The L'Aquila 2009 event was mainly characterised by one main event and although the Emilia 2012 had two large events of similar magnitude, they were quite distant from each other and were thus likely to have impacted different sets of buildings in the database. The Umbria 1997 and Molise 2002 sequences were instead both characterised by two closely situated large events of similar magnitude. The Pollino 1998 case, however, was characterised by one main event and so further investigation into the underestimation of the damage in this case is needed.

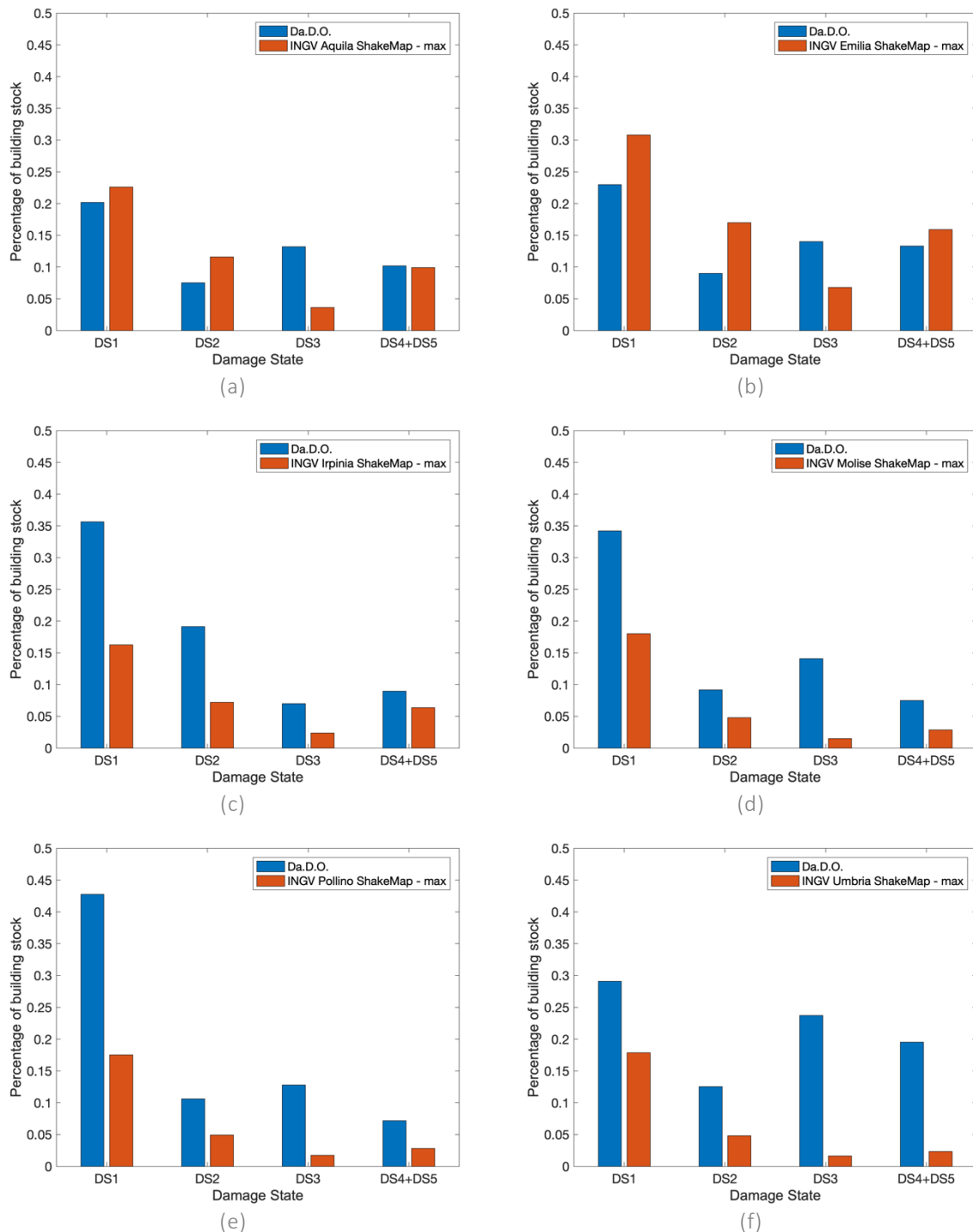


Figure 11. Comparison of observed damage data (Da.D.O.) and estimated damage using the European fragility functions for (a) L'Aquila 2009, (b) Emilia 2012, (c) Irpinia 1980, (d) Molise (2002), (e) Pollino (1998) and (f) Umbria-Marche (1997) [DS1: slight, DS2: moderate, DS3: extensive, DS4: complete, DS5: collapse – note that DS0 (no damage) is not shown on the plots].

It is noted that these tests will need to be repeated once the European fragility functions are finalised and have passed all of the unit tests presented in the previous section.

3.3.3 Greece

Similar tests of the European exposure and fragility models have been undertaken in Greece using two of the most destructive earthquakes of the last decades in Greece, i.e. the Thessaloniki 1978 M_w 6.5 earthquake and the Athens 1999 M_w 5.9 earthquake, for which sufficient data has been collected in order to apply the tests.

Thessaloniki is the second-largest city in Greece, with over 1 million inhabitants in its metropolitan area and the financial centre in Northern Greece. On June 20, 1978 a strong earthquake with magnitude M_w 6.5 occurred with an epicentre located at a distance of about 30km NE of the city. The earthquake caused 47 deaths, 37 of which were due to the collapse of a 9-storey reinforced concrete building, a limited number of partial collapses, and slight to moderate damage to a large number of buildings (Penelis et al., 1988).

Athens is the capital and the largest city of Greece. Athens dominates the Attica region and is one of the world's oldest cities. On September 7, 1999, at 11:56 GMT (14:56 local time), a strong earthquake of magnitude M_w 5.9 occurred very close to Athens, which caused the death of 143 people and the collapse of 100 buildings.

Figure 12 shows the study areas considered in the present study at both national and urban scales.

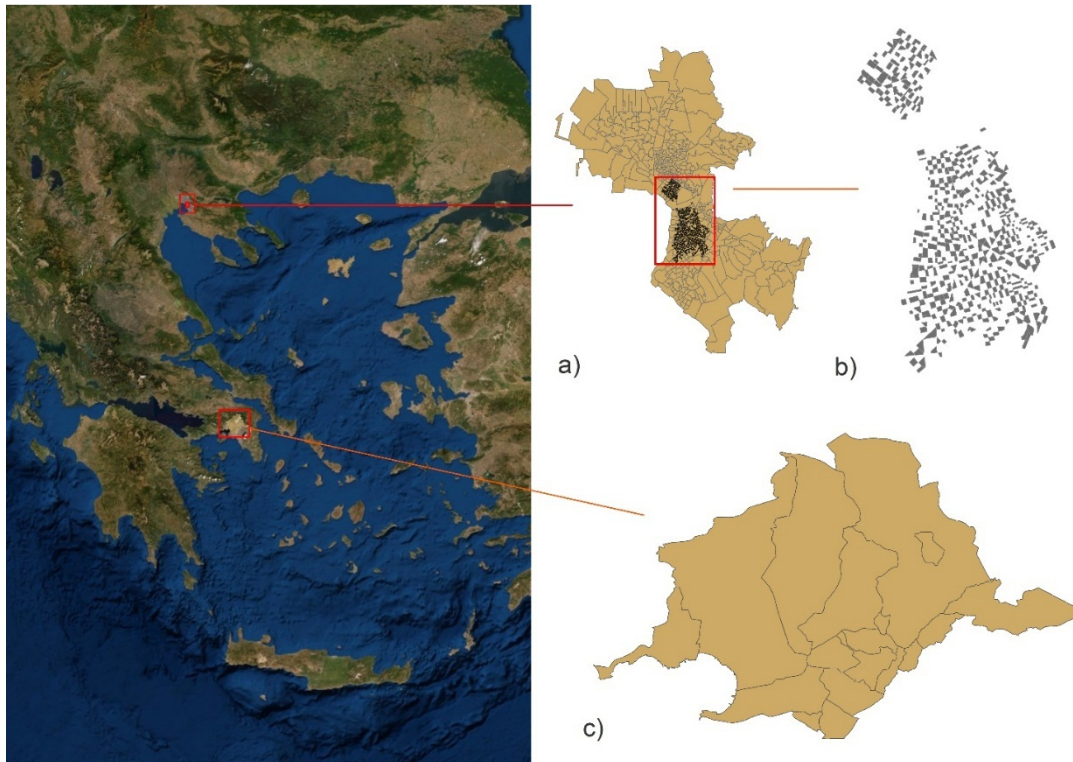


Figure 12. Location of the study area on the map of Greece. (a) Thessaloniki center (in brown) and (b) Earthquake 1978 study area (in black). (c) Athens (Western Attica), Earthquake 1999 study area

To obtain the seismic hazard, the two events were simulated in the OpenQuake-engine as earthquake rupture scenarios using appropriate fault rupture models (Roumelioti et al., 2003; 2007), the ground-motion prediction equation (GMPE) by Akkar and Bommer (2010) and the global slope-based $V_{s,30}$ model of USGS, which has been developed via correlation of $V_{s,30}$ to topographic slope using the methodology proposed by Wald and Allen (2007). In addition, the corresponding USGS ShakeMaps developed after the events were used (<https://earthquake.usgs.gov/data/shakemap/>). Figure 13 compares the PGA values obtained for the two study areas from the scenario analyses with the

OpenQuake-engine using the fault rupture approaches with the respective PGA values from the USGS ShakeMap system.

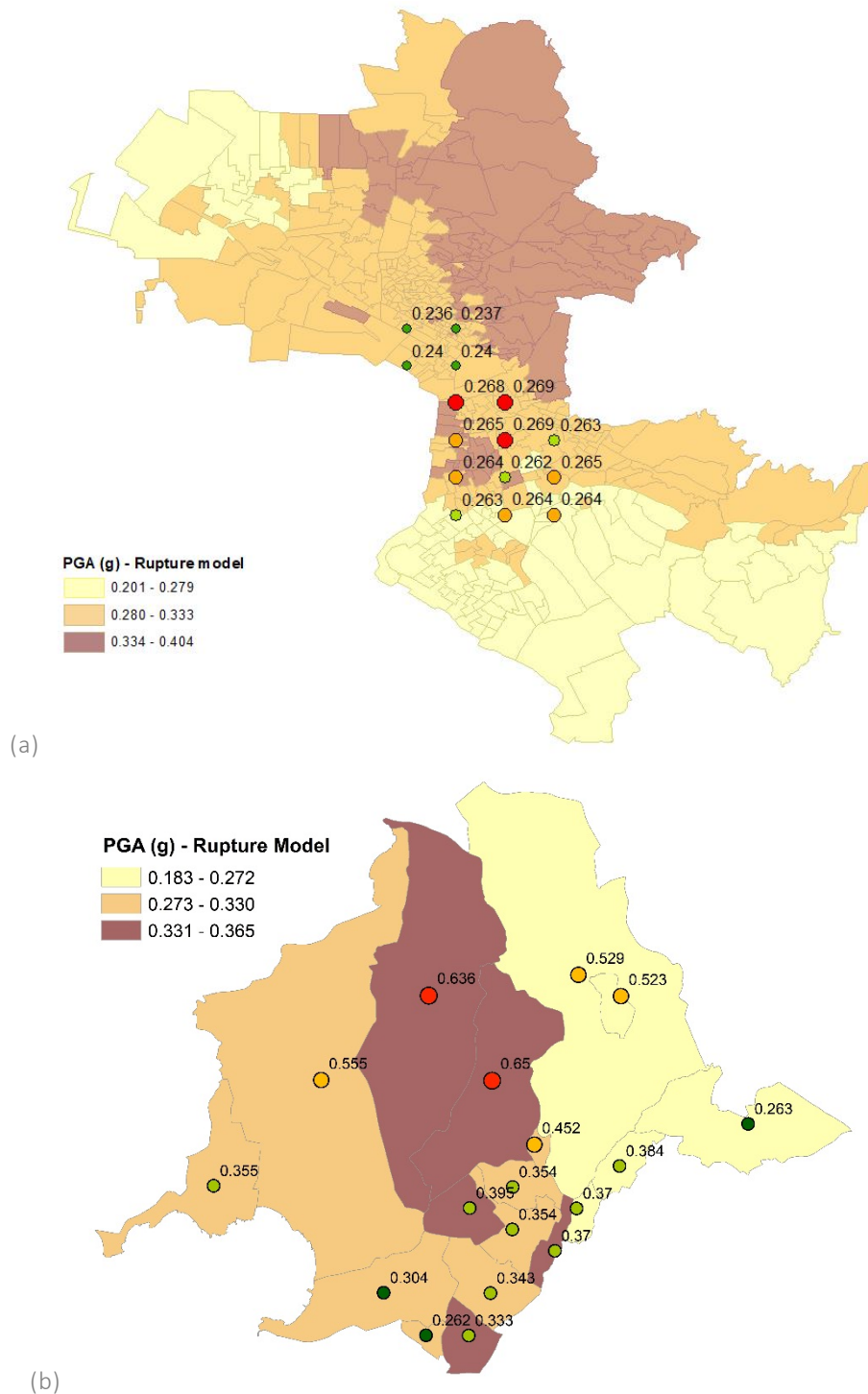


Figure 13. Comparison between PGA values obtained from scenario fault rupture model analysis with the OpenQuake-engine and PGA values from the respective USGS ShakeMap for (a) Thessaloniki 1978 earthquake and (b) Athens 1999 earthquake

For the development of the exposure models, all buildings of Thessaloniki 1978 and Athens 1991 were classified into different building classes following the GEM building taxonomy scheme (Brzev et al., 2013), which allows buildings to be classified according to a number of structural attributes, i.e., main construction material, lateral load resisting system, number of storeys (height) and ductility level, which

is herein assumed to be a function of the construction period and respective seismic design code in force. It is noted that modifications to the GEM taxonomy for the European model were subsequently undertaken (see Deliverable D26.3) and now the design code level and lateral force coefficient are directly used (rather than converted to a ductility level) and so these exposure models will be updated in the future and the tests will be repeated.

For the Thessaloniki exposure model that corresponds to the 1978 situation we used the building inventory developed by Kappos et al. (2008) for the area at the period of the earthquake shown in black in Figure 12b, which is a combination of the 1991 census data, data from previous projects and in-situ work (Milutinovic and Trendafiloski, 2003; Kappos et al., 2008). The inventory includes 8800 buildings for which detailed damage records are available. For the Athens exposure model that corresponds to the 1999 situation we used the 2011 building census data, after removal of all buildings constructed after 1999. The exposure model that was developed includes 96,606 residential buildings. Figure 14 shows the main building typologies of the adopted Thessaloniki and Athens exposure models following the GEM building taxonomy. Over 55% of the buildings in Thessaloniki study area are low-code reinforced concrete structures, with dual lateral load-resisting system and number of storeys above ground larger than three, whereas in the Athens study area the most frequent building classes concern low-code reinforced concrete infilled frames, with number of storeys above ground from one to five.

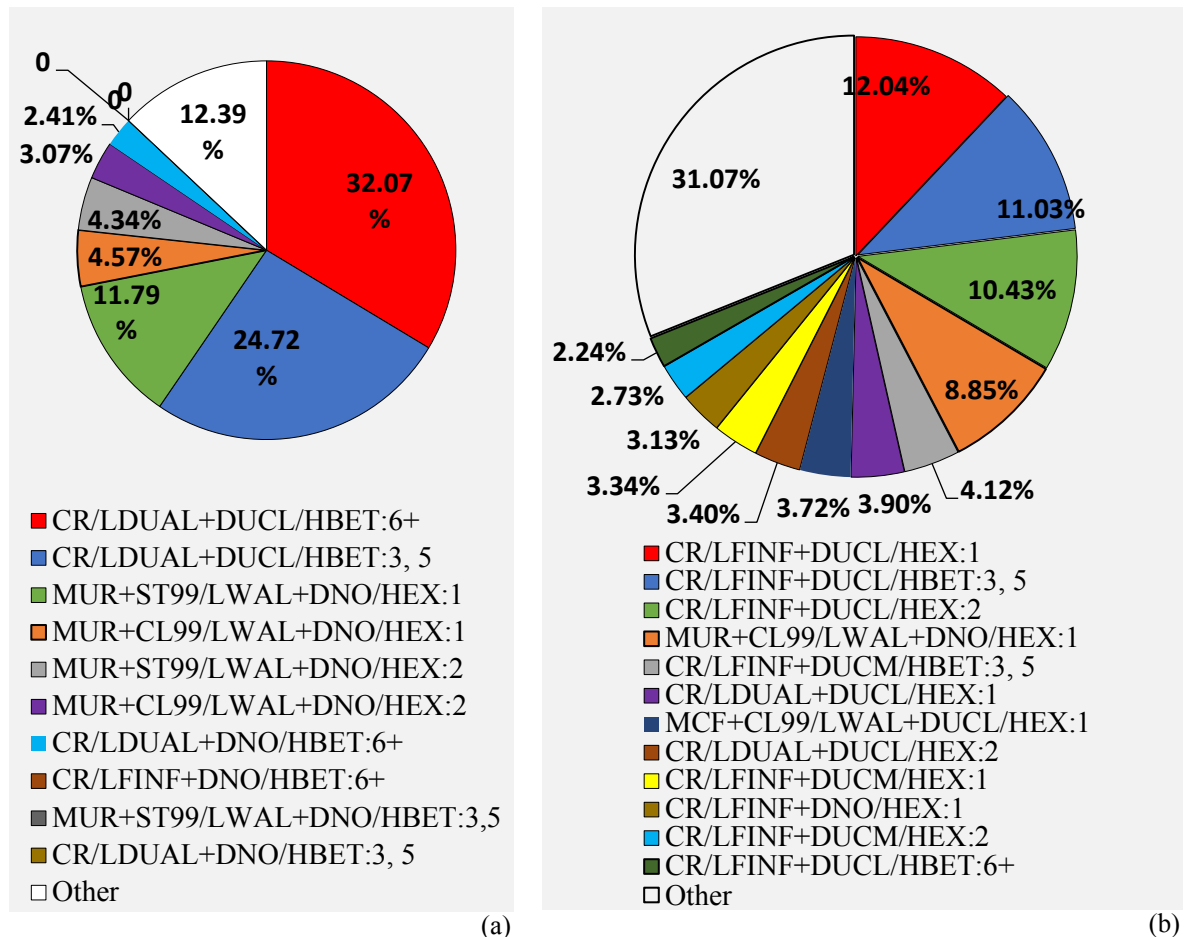


Figure 14. Most common taxonomies in (a) Thessaloniki 1978 and (b) Athens 1999.

For the vulnerability analysis, the GEM fragility models (Martins and Silva, 2018) were adopted as the European fragility functions (based on the methodology of Deliverable D26.5) were not available at the

time this work was undertaken. However, it is noted that once the exposure model has been updated, the building classes will be mapped to the latest European fragility functions and these tests will be repeated.

To estimate the expected damages to the buildings located in the study areas of Thessaloniki and Athens, for the Thessaloniki 1978 and the Athens 1999 earthquakes respectively, the ‘Scenario Damage Calculator’ and the ‘Scenario from ShakeMap Calculator’ (Silva and Horspool, 2019) of the OpenQuake-engine were used. Figure 15 shows the distribution of the expected damage states of residential buildings in Athens and Thessaloniki for the scenario damage analysis using the fault rupture models and the USGS ShakeMaps. For both Athens and Thessaloniki case studies, irrespectively of the seismic hazard model (rupture model and USGS ShakeMap), the damages are generally in good correlation, with the rupture model, which is a priori more accurate, leading to slightly higher damages. For the Athens case study, higher damages are found predominantly in the northern parts of the study area, closer to the epicentre, where higher seismic demands are found.

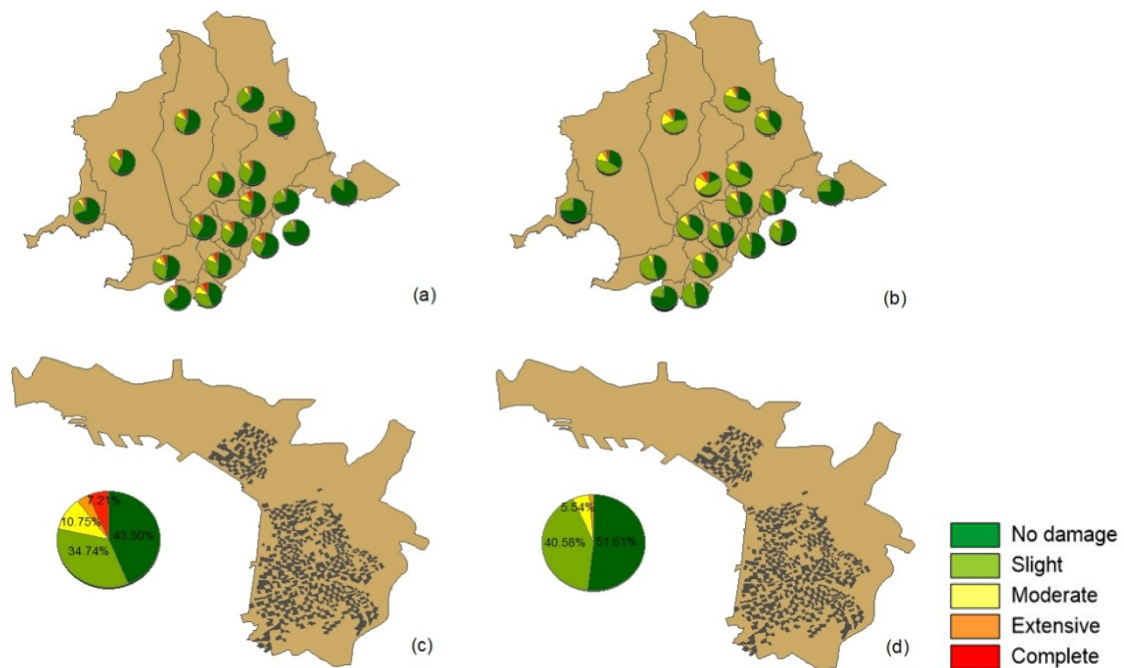


Figure 15. Distribution of expected damage states of residential buildings obtained from scenario analysis with OpenQuake for: (a) Athens 1999 earthquake using the fault rupture model, (b) the Athens 1999 earthquake using the USGS ShakeMap, (c) Thessaloniki 1978 earthquake using the fault rupture model, (d) Thessaloniki 1978 earthquake using the USGS ShakeMap.

The predicted earthquake damages with the two approaches are finally compared with the actual damages observed in the study areas after the 1978 Thessaloniki (Kappos et al., 2008) and the 1999 Athens (ESYE, 1999) earthquakes (Table 1 and Table 2). The results are correlated well with the observed damages (Green: No reduction of seismic capacity. Yellow: Reduced seismic capacity. Usage not permitted before repair and strengthening. Red: Unsafe. Usage or entry is prohibited.). The five damage states from the analytically predicted damages have been reduced to the three damage states of the recorded damages in the way shown in the Tables 1 and 2. The comparison in the case of Thessaloniki study area is exceptionally good, with differences about only 5%, in particular when using the rupture model. This should be expected as the Thessaloniki exposure model has less uncertainties (i.e. use of 1991 census data in combination with data from previous projects and in-situ inspection work just after the earthquake) compared to the Athens exposure model, which is only based on an adjusted 2011 building census data.

Table 1. Comparison of observed and estimated damage for the Thessaloniki 1978 earthquake

DAMAGE STATE	OBSERVED DAMAGES COLOR TAG	ESTIMATED DAMAGE – FAULT RUPTURE MODEL	ESTIMATED DAMAGE – USGS SHAKEMAP	OBSERVED DAMAGE – POST EARTHQUAKE TAGGING
NO DAMAGE SLIGHT	Green	78.2 %	92.2 %	74.5 %
MODERATE EXTENSIVE	Yellow	14.6 %	6.95 %	19.1 %
COMPLETE	Red	7.2 %	0.85 %	6.4 %

Table 2. Comparison of observed and estimated damage for the Athens 1999 earthquake

DAMAGE STATE	OBSERVED DAMAGES COLOR TAG	ESTIMATED DAMAGE – FAULT RUPTURE MODEL	ESTIMATED DAMAGE – USGS SHAKEMAP	OBSERVED DAMAGE – POST EARTHQUAKE TAGGING
NO DAMAGE SLIGHT	Green	82.8 %	83.7 %	62.5 %
MODERATE EXTENSIVE	Yellow	11.2 %	13.1 %	32.8 %
COMPLETE	Red	6.0 %	3.2 %	4.7 %

4 System Tests

This is the first level in which the complete ESRM20 model is tested as a whole. As mentioned previously, the latest European hazard model (ESHM20) is not available and so the tests presented herein, which focus on the impact of the resolution of the exposure on the losses, have made use of the ESHM13 source model together with the ESHM20 ground motion and site model (see Deliverable D26.4).

The main reason for testing the exposure resolution is to investigate whether the current resolution is appropriate in terms of the main risk metrics that will be provided with ESRM20, i.e. national AAL and loss exceedance curves and sub-national AAL at the first administrative level. Another aspect which will be investigated in the future relates to time required to run higher resolutions of exposure (on a server with given technical characteristics). The latter has not yet been undertaken as the calculations have so far been run on different servers. Finally, additional workflows in terms of the modelling of the coordinates of the buildings and site conditions (see Section 4.2) will be undertaken. Hence, the initial study presented herein will continue to be expanded until the final release of the ESRM20 (and beyond, as part of the Horizon 2020 RISE project: <http://rise-eu.org/home/>).

4.1 Resolution of Exposure Models

As described in SERA Deliverable D26.3 and Crowley et al. (2020), the European exposure model is developed for different resolutions across Europe as a function of the datasets used to develop the model (typically census data). Table 3 summarises the resolution (in terms of administrative boundaries) at which each exposure model has been developed for the residential, industrial and commercial buildings. The average area of administrative boundaries is presented in Figure 16.

Table 3. Administrative boundary resolution for the residential, industrial and commercial exposure models

COUNTRY	RESIDENTIAL	COMMERCIAL	INDUSTRIAL
ALBANIA	Adm3	Adm1	Gridded 1x1 km ²
ANDORRA	Adm1	Adm1	Adm1
AUSTRIA	Adm1	Adm1	Gridded 1x1 km ²
BELARUS	Adm2	Adm1	Adm1
BELGIUM	Adm4	Adm2	Gridded 1x1 km ²
BOSNIA AND HERZEGOVINA	Adm3	Adm3	Gridded 1x1 km ²
BULGARIA	Adm2	Adm1	Gridded 1x1 km ²
CROATIA	Adm2	Adm2	Gridded 1x1 km ²
CYPRUS	Adm2	Adm1	Gridded 1x1 km ²
CZECHIA	Adm2	Adm1	Gridded 1x1 km ²
DENMARK	Adm2	Adm2	Gridded 1x1 km ²
ESTONIA	Adm1	Adm1	Gridded 1x1 km ²
FINLAND	Adm2	Adm2	Gridded 1x1 km ²
FRANCE	Adm5	Adm2	Gridded 1x1 km ²
GERMANY	Adm4	Adm3	Gridded 1x1 km ²
GIBRALTAR	Adm0	Adm0	Adm0
GREECE	Adm3	Adm3	Gridded 1x1 km ²
HUNGARY	Adm1	Adm1	Gridded 1x1 km ²
ICELAND	Adm2	Adm1	Gridded 1x1 km ²

COUNTRY	RESIDENTIAL	COMMERCIAL	INDUSTRIAL
IRELAND	Adm1	Adm1	Gridded 1x1 km ²
ISLE OF MAN	Adm1	Adm0	Adm2
ITALY	Adm3	Adm3	Gridded 1x1 km ²
KOSOVO	Adm2	Adm2	Adm2
LATVIA	Adm1	Adm1	Gridded 1x1 km ²
LIECHTENSTEIN	Adm1	Adm1	Adm1
LITHUANIA	Adm2	Adm1	Gridded 1x1 km ²
LUXEMBOURG	Adm2	Adm2	Gridded 1x1 km ²
MALTA	Adm1	Adm1	Gridded 1x1 km ²
MOLDOVA	Adm1	Adm1	Gridded 1x1 km ²
MONACO	Adm0	Adm0	Gridded 1x1 km ²
MONTENEGRO	Adm1	Adm1	Gridded 1x1 km ²
NETHERLANDS	Adm2	Adm1	Gridded 1x1 km ²
NORTH MACEDONIA	Adm1	Adm1	Gridded 1x1 km ²
NORWAY	Adm2	Adm1	Gridded 1x1 km ²
POLAND	Adm2	Adm1	Gridded 1x1 km ²
PORTUGAL	Adm3	Adm3	Gridded 1x1 km ²
ROMANIA	Adm2	Adm1	Gridded 1x1 km ²
SERBIA	Adm2	Adm2	Gridded 1x1 km ²
SLOVAKIA	Adm2	Adm2	Gridded 1x1 km ²
SLOVENIA	Adm2	Adm2	Gridded 1x1 km ²
SPAIN	Adm2	Adm1	Gridded 1x1 km ²
SWEDEN	Adm2	Adm2	Gridded 1x1 km ²
SWITZERLAND	Adm3	Adm1	Gridded 1x1 km ²
TURKEY	Adm1	Adm1	Adm1
UKRAINE	Adm2	Adm1	Adm1
UNITED KINGDOM	Adm2	Adm1	Gridded 1x1 km ²

Based on the information presented in this section, the following countries have been identified as priority countries to check the impact of the resolution on the risk results given their low resolution and their range of levels of hazard: Turkey, Spain, Iceland, Bulgaria, Albania, Austria and Hungary, Belarus and United Kingdom.

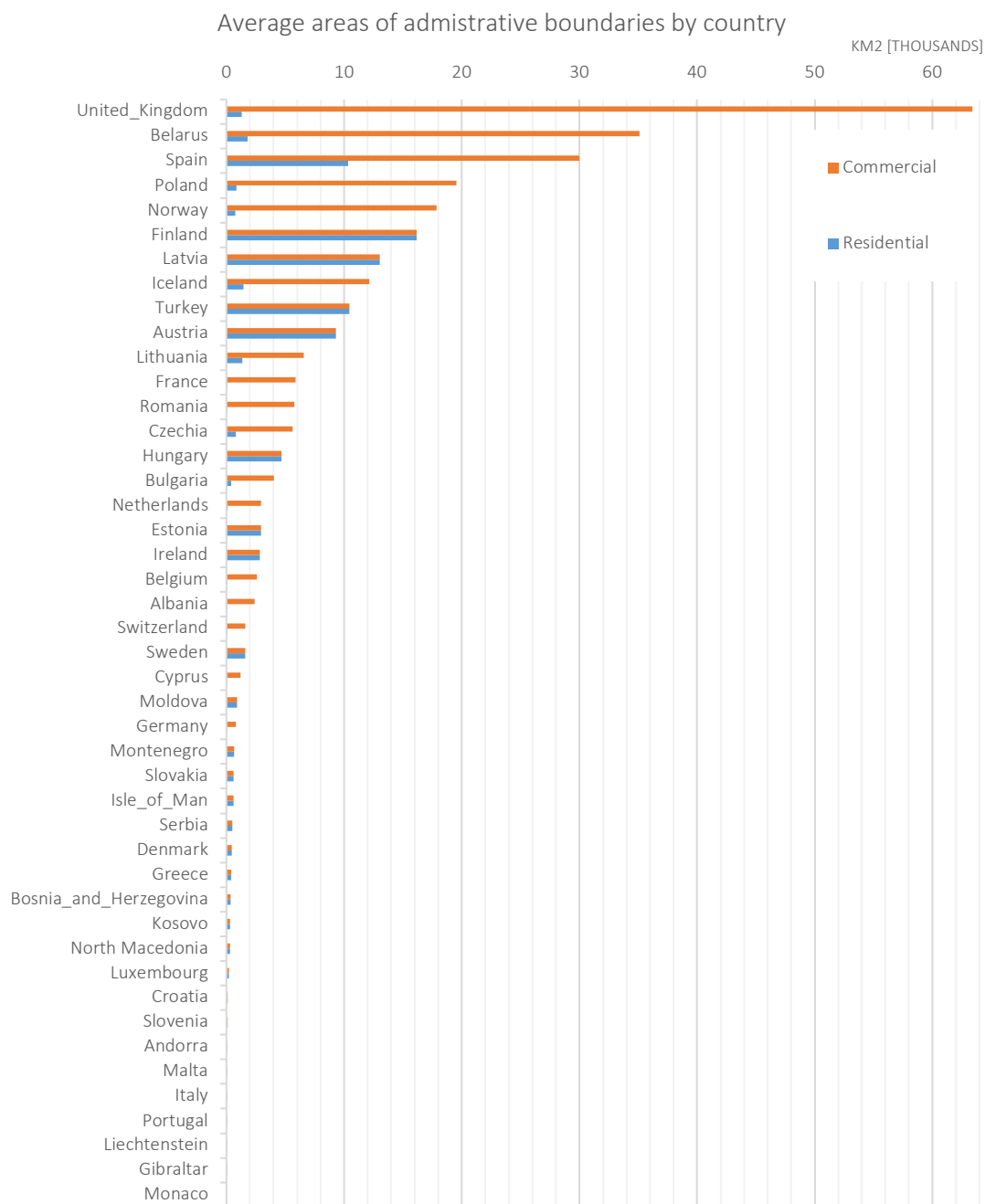


Figure 16. Average administrative area per country and occupancy

4.2 Disaggregation of the Exposure Model

Exposure resolution is tested for several modelling options, including different geographical representations (i.e., administrative and gridded distributions). As commonly known, the uncertainty in the location of assets introduces a bias in the level of ground shaking and, consequently, the level of damage. Moreover, the bias can be magnified by the various site conditions at different locations. This is investigated by testing the initial cases presented in Table 4.

Table 4. Exposure testing cases

EXPOSURE TYPE	CASES	LOCATION	SITE PROPERTIES
GRIDDED	30, 60, 120, 240, 480 and 960 arcsec *	even grids of points	closest point
ADMINISTRATIVE	workflow 1 (wf1)	boundary centroid	closest point
	workflow 2 (wf2)	boundary centroid	average (weighted by the density of built-up areas)
	workflow 3 (wf3)	maximum density of built-up areas	average (weighted by the density of built-up areas)

* squared grids with areas equivalent to 1, 4, 16, 64, 256, 1024 km²

It is noted that other workflows will be considered in future work – for example, the average site properties (weighted by the density of built-up areas) will be considered with the gridded exposure models, and the weighted mean centroid will also be considered for the location of the administrative exposure models.

For the gridded exposure, residential, commercial and industrial occupancies are disaggregated to six resolutions 30, 60, 120, 240, 480 and 960 arcsec (30 arcsec equals to approximately 1km at the equator). In this process, buildings are redistributed using remote sensing information at 38x38m resolution and then aggregated to the different grids, as demonstrated in Figure 17. More details on the disaggregation methodology can be found in Dabbeek and Silva (2020), the datasets used for exposure disaggregation include:

- Global Human Settlement Layer (GHSL-Pesaresi et al. 2015)
Raster dataset with global coverage, it maps built-up areas with a resolution of 38x38m. This dataset was used primarily to locate buildings.
- Corine Land Cover (CLC-Feranec et al. 2016)
Raster dataset at the European level, it includes 47 land classes with a resolution of 100x100m. This dataset was used to separate the locations of residential and other occupancies (commercial and industrial).
- Night light time (Román et al. 2018)
Raster dataset with global coverage, it indicates the intensity of reflected light during night-time at the resolution of 500x500m. This dataset is used for countries not covered by CORINE (e.g., Belarus). In specific, nightlights are used to map commercial/industrial regions, as studies indicate a strong correlation between night-time lights and economic activity.

For the administrative exposure case, workflows 1 and 2 are identical in terms of assets location (boundary centroid), but different in terms of site properties. In the latter case, the site parameters (V_{S30} , slope and geological category) represent the average weighted by the density of built-up areas within the respective administrative boundary. In workflow 3, locations represent the maximum built-up density, and site parameters are determined from the weighted average of the built-up areas. Figure 18 illustrates the difference in the location between the three workflows for Turkey.

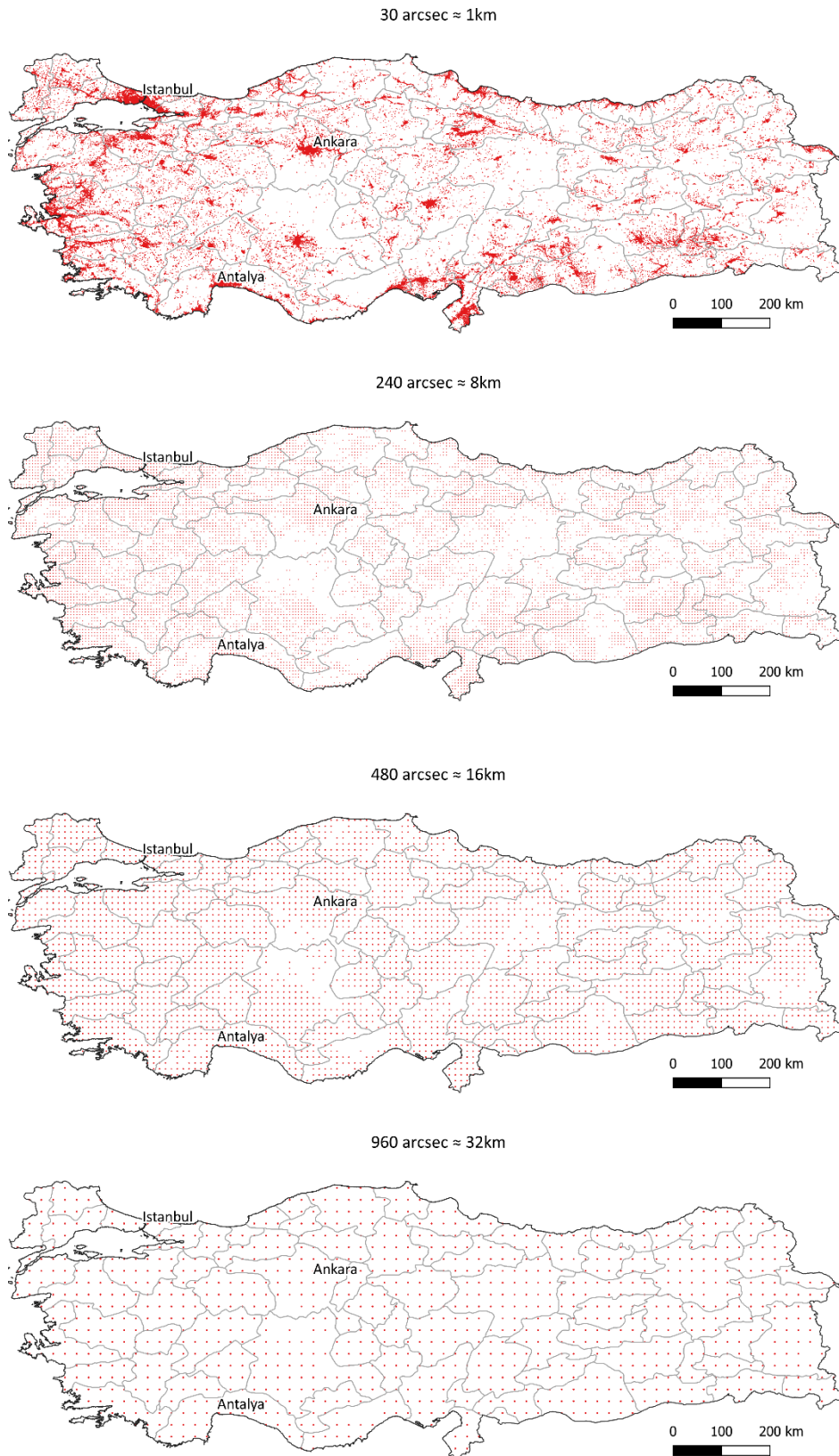


Figure 17. Gridded exposure for Turkey at 30, 240, 480 and 960 arcsec resolution.

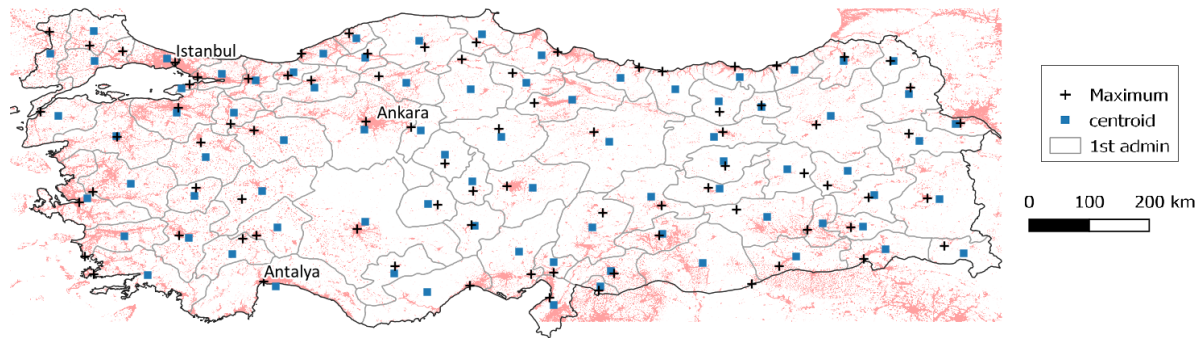


Figure 18. Exposure locations for the administrative workflows.

4.3 Testing Exposure Model Resolution

The impact of the resolution of exposure models has been tested for AAL and losses per return periods at the national and the first sub-national level of ESRM20.

4.3.1 National level

AAL

The risk metrics are calculated using 100,000 years of hazard investigation time for all modelling cases. Figure 19 presents the change in the AAL's between the different exposure modelling cases and the benchmark model (30 arcsec). For the gridded exposure, the results indicate relatively stable losses up 240 resolution with a maximum difference of 3%. After this, the results become inaccurate, reaching a maximum difference of 25%, which can be seen in the case of Iceland and Turkey. The analysis illustrates that at the national level, the AAL is better estimated with wf2. The analysis is extended to the sub-national level in the following sections. Notably, the percentage change is likely to be proportional to the size of the administrative boundary, population distribution and the attenuation of ground motions and plots to demonstrate this will be produced in future versions of the study.

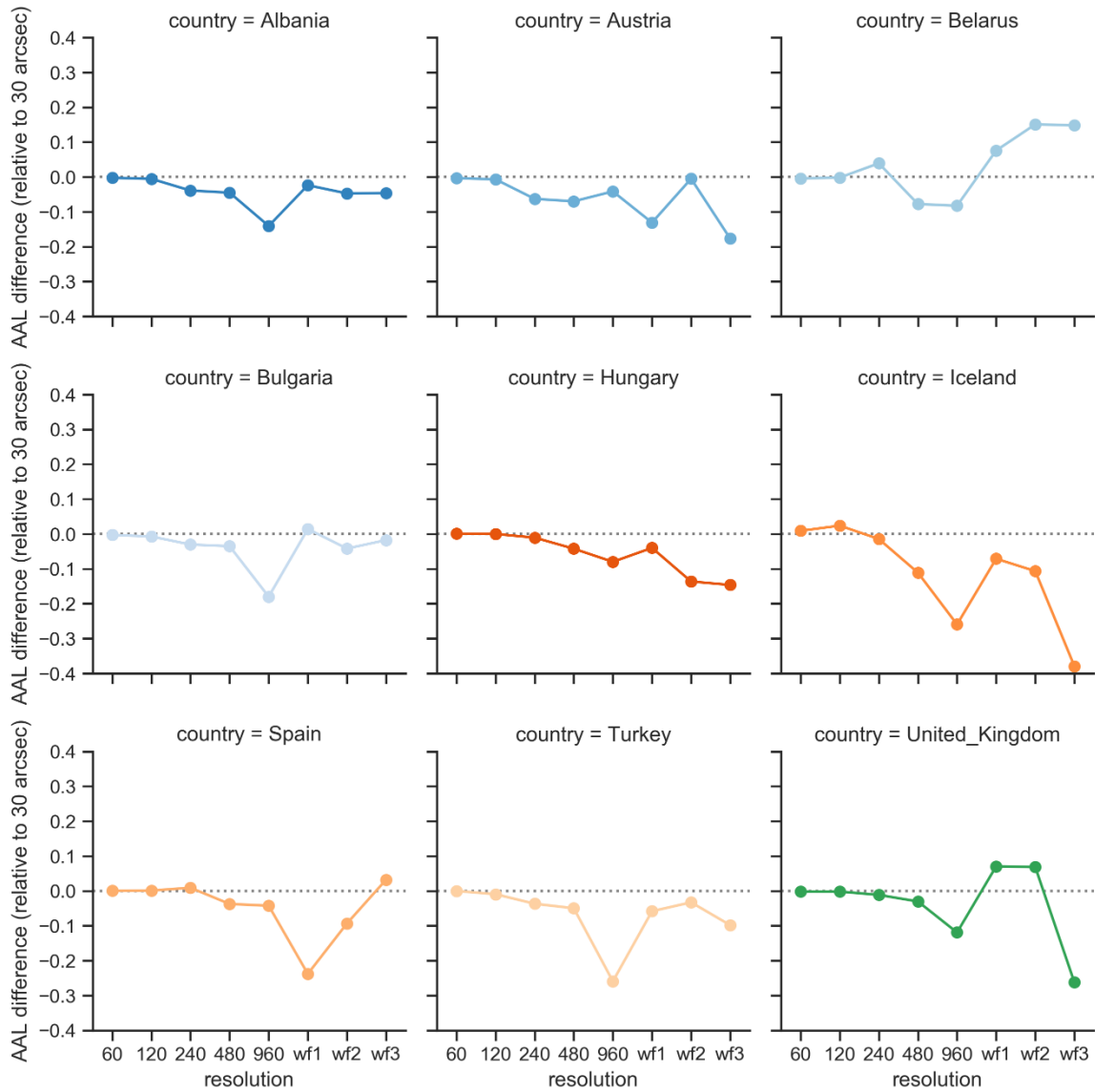


Figure 19. AAL change relative to the benchmark case (30 arc-second exposure) for nine countries.

Losses per return periods

Exposure resolution is also tested for specific return periods, including 50, 100, 200, 500 and 1000 years return period. Figure 20 illustrates a similar trend to that observed in the AAL case, where the level of bias becomes more evident at lower resolutions (480, 960 and admin 1). It can be observed that the losses of the frequent return periods (50, 100) are more affected by the resolution. Generally, smaller events lead to ground shaking that covers smaller regions and thus any shift of the location of the assets can change the level of shaking dramatically. Also, there is a high sensitivity of small numbers to change. The change in resolution tends to create a positive relative difference in the losses for the longer return periods. This is likely to be due to the fast attenuation of ground motions under large events. By aggregating the assets, all buildings in the portfolio at a given distance are given the same level of ground motion, whereas in disaggregated exposure models the assets would have varying levels of ground shaking. The impact of moving the exposure caused by portfolio aggregation is not linear: shifting one asset towards the source has a larger (positive) impact on the losses than shifting it away from the source. This can clearly be seen in the countries with higher levels of hazard (e.g. Turkey, Albania, Iceland, Spain).

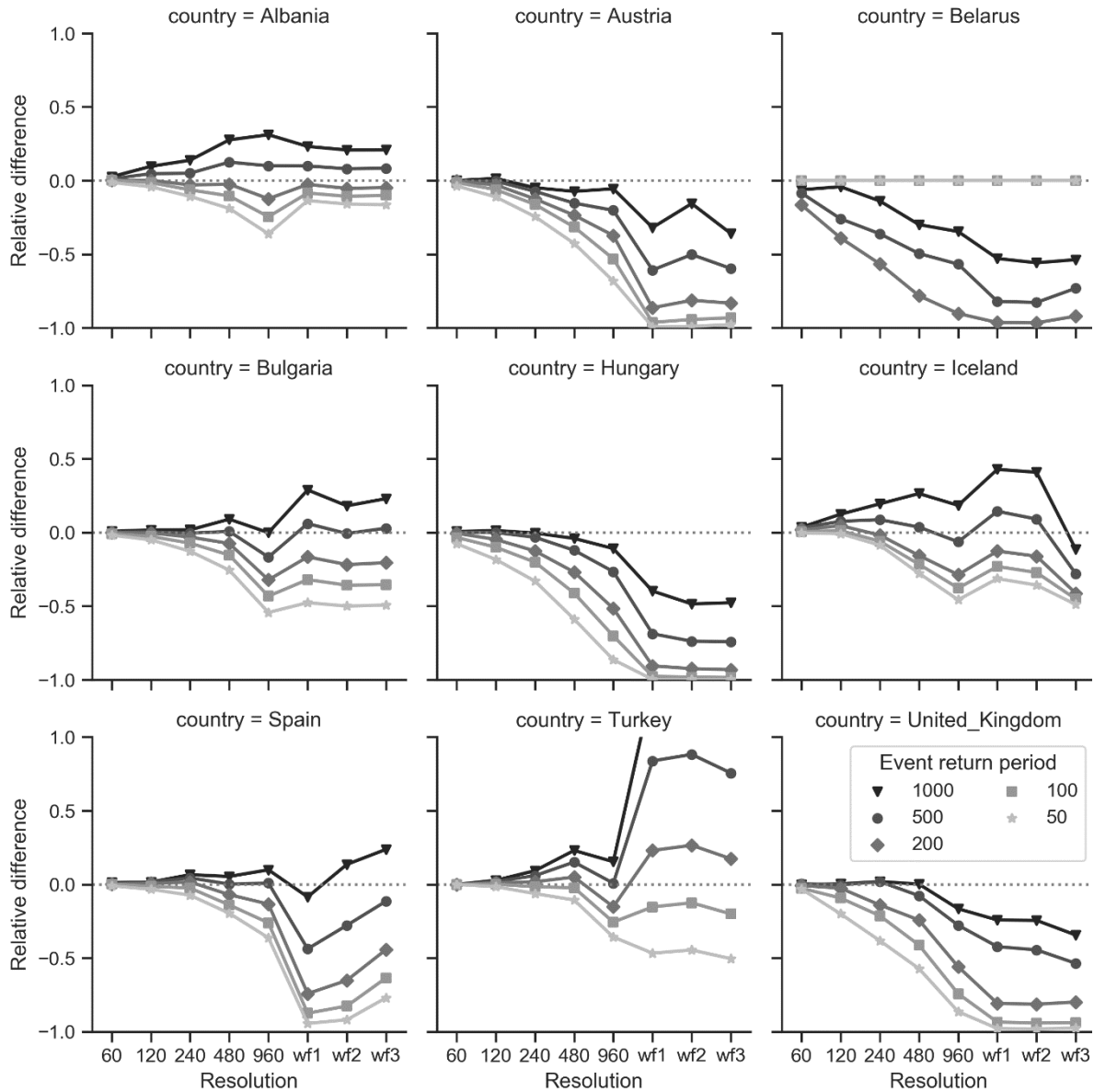


Figure 20. Relative differences in return periods losses given different resolutions compared to the benchmark case (30arcsec).

Another aspect of exposure testing included the occupancy class (residential, commercial and industrial). As demonstrated in Table 3, the resolutions differ between occupancies. Generally, commercial exposure has lower resolution compared to the residential. Figure 21 illustrates the difference in the losses by occupancy class. For the case of Belarus, commercial and industrial exposure is at the 1st admin-level, where the results are overestimated by 70%. One reason for this significant difference is the large boundaries (on average 35,000 km² per region). The second reason occurs as the commercial and industrial assets are typically clustered, while residential assets are more spread (which can be identified from CORINE land cover classes⁴). Consequently, the results are more sensitive for commercial and industrial exposure.

⁴ <https://land.copernicus.eu/pan-european/corine-land-cover>

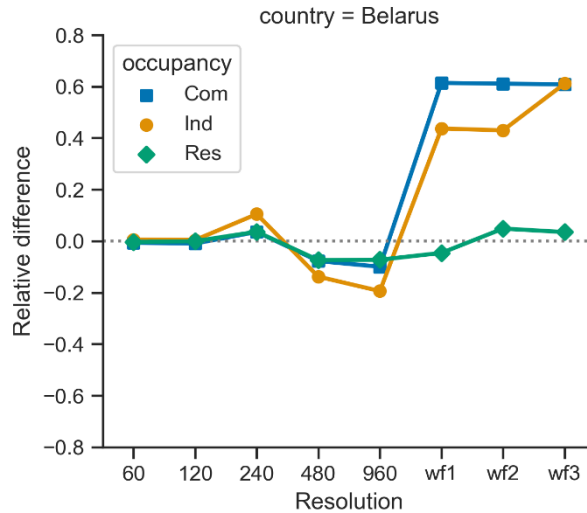


Figure 21. Change in the AAL by occupancy class in Belarus.

4.3.2 Sub-national level

The impact of exposure resolution is also tested by presenting the results at the sub-national level (1st admin)⁵. The results in Figure 22 presents the change in the AAL at the 1st admin level (for six capital regions). The results indicate higher uncertainty in AAL at the subnational level than that observed at the national level (see Figure 19). It is worth mentioning that ground motion spatial correlation is not yet considered here at any level of resolution.

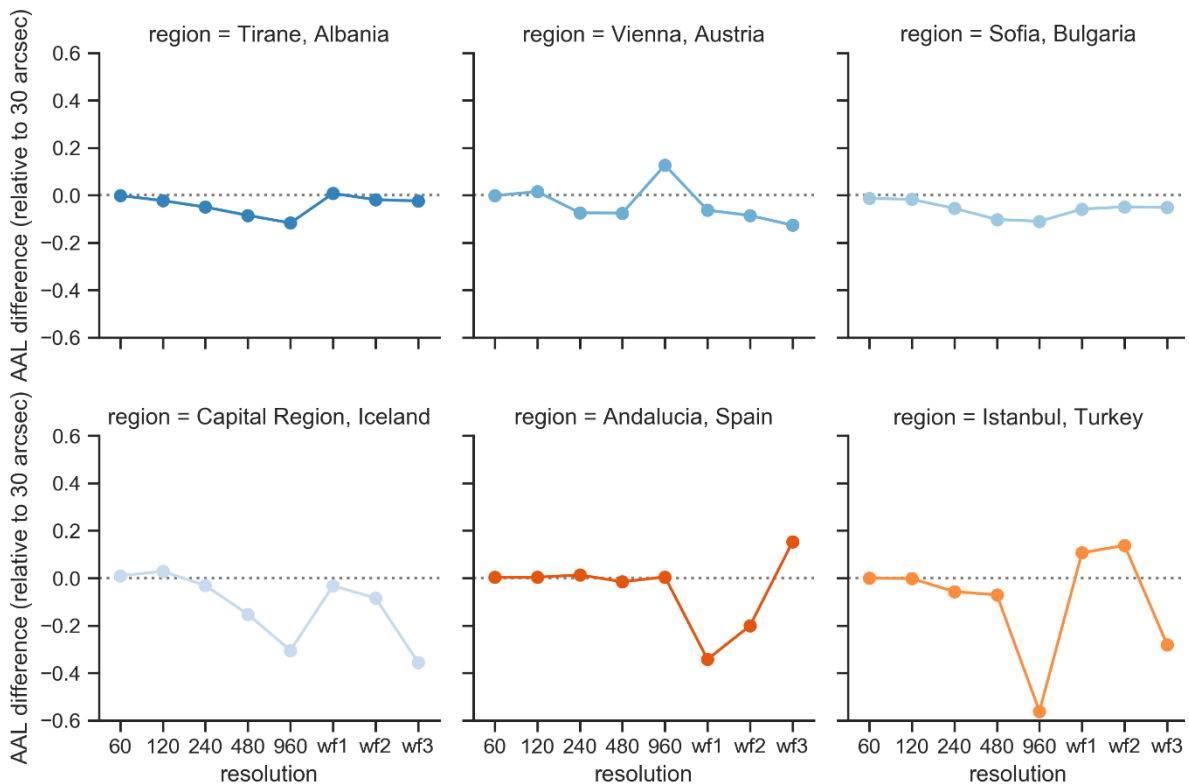


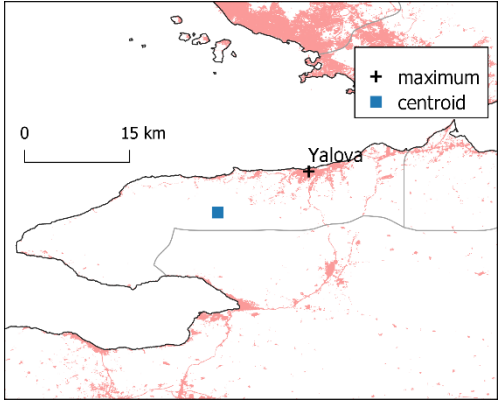
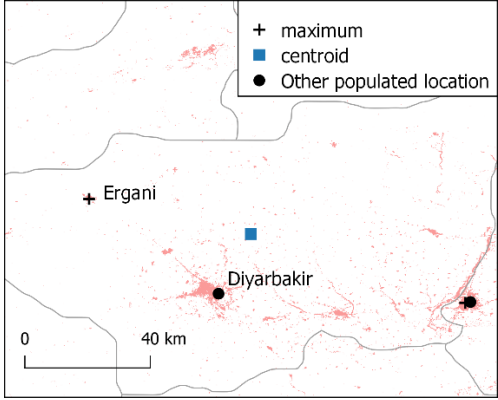
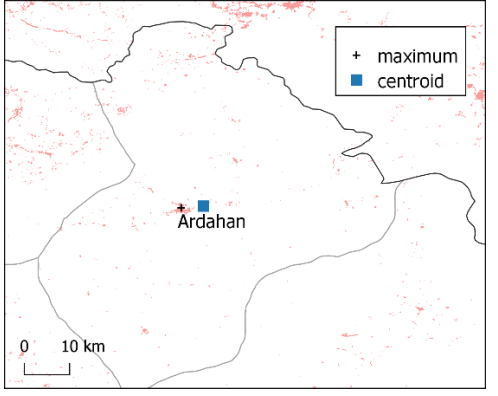
Figure 22. AAL change relative to the benchmark case (30 arc-second exposure) at the 1st Admin level.

⁵ It is noted that the resolution of wf1, wf2 and wf3 corresponds to that presented previously in Table 3 for each country, but the results are aggregated and presented at the first administrative level.

4.4 Remarks on the Exposure Resolution

Improving exposure spatial resolution for aggregated portfolios can minimize the bias in the estimation of losses. In particular, resolutions between 120 to 240 arc-seconds appear to provide a reasonable trade-off between accuracy and computational demand. The improvements from disaggregating to high-resolution (e.g., 30 arc-seconds) was insignificant; therefore, it is currently considered as an unjustified effort for the European risk model. Concerning using the different administrative workflows (wf1, wf2 and wf3), at the national level, wf2 seemed to provide more accurate estimates. Moreover, it was found that at the sub-national level, using wf2 or wf3 can provide better estimates for the AAL. Specifically, in 70% of the regions (out of 188 regions analysed here), wf2 and wf3 provided more accurate AAL's than wf1. It should be noted that there is no ideal workflow due to exposure randomness. Yet the second workflow (simple centroid with average site parameters) performed better in a larger number of regions and provided relatively more accurate estimates for the AAL. Some of the drawbacks and advantages of using the different workflows are illustrated in Table 5. As mentioned previously, these analyses will continue until the release of ESRM20 and the final outcome of the studies will be presented in the academic literature.

Table 5. Performance of admin workflows in Turkey.

Region	Difference in the AAL [%]			Comment
	wf1	wf2	wf3	
	30	11	0.4	Regions with exposure concentrated in one location are better represented by the maximum centroid method
	11	7	270	Regions with more than one populated place, are not well presented by the maximum centroid method
	2	21	18	In this case, exposure locations are similar. In terms of site conditions, the closest point method performed better than the average. This difference could be a result of hazard distribution over the region

5 Acceptance Testing

The final level of testing is conducted to determine whether the system is ready for release. Once all of the tests presented in the previous Chapters have been completed and the components of the ESRM20 are finalised, acceptance tests will be initiated. A workshop to investigate a wide range of results of the ESRM20 with an audience of experienced risk modellers (some of whom will also be end-users/stakeholders) is planned before the release of the model. Comparisons of the results will also be made against other initiatives that have covered European risk such as the Global Assessment Report (GAR, 2015), GEM's Global Risk Map v2018.1 (GEM, 2018; Silva et al., 2020) as well as national risk assessments and insurance/reinsurance industry models (where available). In preparation for these acceptance tests, some of this testing data has been collected and is presented in the following sections.

5.1 National Risk Assessments

Italy's 2018 National Risk Assessment (NRA) by the Department of Civil Protection⁶ provides a number of results against which the Italian residential building results in the ESRM20 should be compared. Figure 23 shows the map of the average annual direct economic loss calculated for each region in Italy. The total national annual average direct economic loss has been estimated to be in the order of 2 Billion Euro (or 0.063% of the replacement cost of residential buildings). The average annual number of fatalities has been calculated as 500.

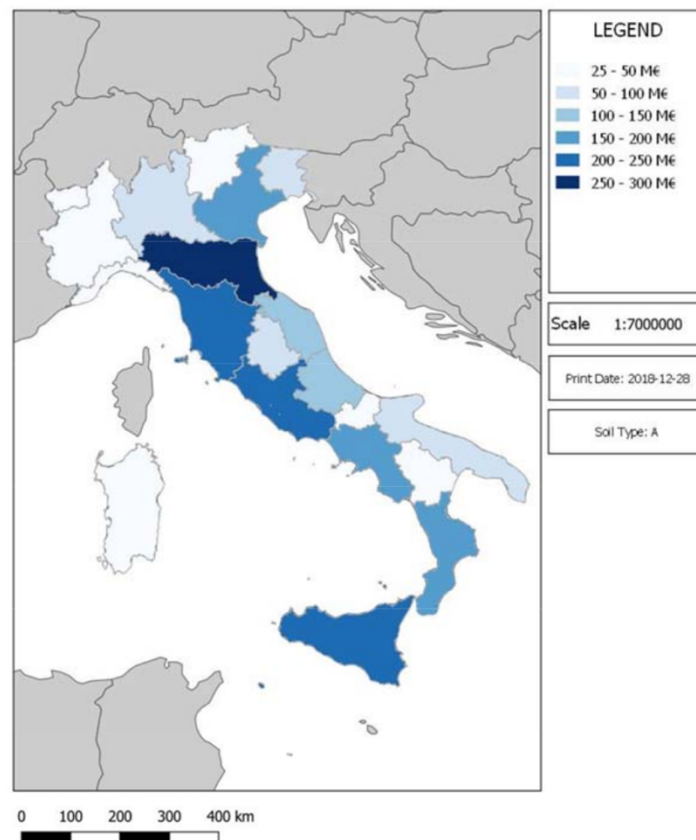


Figure 23. Map of average annual direct economic loss for the regions in Italy⁴

⁶ <http://www.protezionecivile.gov.it/documents/20182/823803/Documento+sulla+Valutazione+nazionale+dei+rischi/>

5.2 Global Earthquake Model

The values of AAL and AALR for each European country in GEM's 2018.v1 risk model (GEM, 2018; Silva et al., 2020) is provided in Table 6. It is noted that these calculations used a v0.1 of the European exposure model (see Deliverable D26.3), the ESHM13 hazard model (Woessner et al., 2013), site amplification through the use V_{s30} inferred from topography (Wald and Allen, 2007) and the Martins and Silva (2018) vulnerability models. Any large differences between these values and the ESRM20 values will need to be investigated and clearly explained and justified.

Table 6. AAL and AALR (GEM's 2018.v1 model)

COUNTRY	AAL [MILLION USD]	AALR [%]
ALBANIA	34	0.11
ANDORRA	0	0.00
AUSTRIA	141	0.01
BELARUS	0	0.00
BELGIUM	94	0.01
BOSNIA AND HERZEGOVINA	14	0.02
BULGARIA	139	0.04
CROATIA	58	0.03
CYPRUS	110	0.09
CZECHIA	6	0.00
DENMARK	7	0.00
ESTONIA	1	0.00
FINLAND	0	0.00
FRANCE	212	0.00
GERMANY	195	0.00
GIBRALTAR	0	0.00
GREECE	560	0.09
HUNGARY	23	0.01
ICELAND	41	0.06
IRELAND	0	0.00
ITALY	3,586	0.06
KOSOVO	8	0.04
LATVIA	1	0.00
LIECHTENSTEIN	1	0.01
LITHUANIA	1	0.00
LUXEMBOURG	1	0.00
MALTA	2	0.01
MOLDOVA	23	0.04
MONACO	1	0.02
MONTENEGRO	9	0.03
NETHERLANDS	71	0.00
NORTH MACEDONIA	23	0.05
NORWAY	8	0.00
POLAND	7	0.00
PORTUGAL	73	0.01
ROMANIA	228	0.06
SERBIA	64	0.02
SLOVAKIA	38	0.01
SLOVENIA	30	0.03
SPAIN	103	0.00

COUNTRY	AAL [MILLION USD]	AALR [%]
SWEDEN	5	0.00
SWITZERLAND	94	0.01
TURKEY	1,379	0.15
UNITED KINGDOM	54	0.00

5.3 Global Assessment Report (GAR)

GEM's 2018.v1 risk model has been compared against the values from GAR (2015) (see Silva et al., 2020) and so this provides another source of AAL and AALR data that should be considered when undertaking acceptance tests of the ESRM20. The values for the European countries in ESRM20 are presented in Table 7.

Table 7. AAL and AALR from the GAR (2015) model

COUNTRY	CAPITAL STOCK [MILLION USD]	AAL [MILLION USD]	AALR [%]
ALBANIA	40,460	47	0.12
ANDORRA	8,382	0	0.00
AUSTRIA	1,801,472	525	0.03
BELARUS	229,400	0	0.00
BELGIUM	1,980,551	190	0.01
BOSNIA AND HERZEGOVINA	30,656	15	0.05
BULGARIA	163,822	83	0.05
CROATIA	188,114	153	0.08
CYPRUS	71,611	29	0.04
CZECHIA	1,007,263	150	0.01
DENMARK	1,346,393	3	0.00
ESTONIA	79,617	1	0.00
FINLAND	965,383	1	0.00
FRANCE	10,329,419	501	0.00
GERMANY	15,114,873	2,350	0.02
GIBRALTAR	4,042	3	0.06
GREECE	1,181,283	5,109	0.43
HUNGARY	562,480	123	0.02
ICELAND	57,292	32	0.05
IRELAND	778,822	13	0.00
ITALY	8,604,332	9,773	0.11
LATVIA	95,609	0	0.00
LIECHTENSTEIN	18,837	10	0.05
LITHUANIA	135,614	1	0.00
LUXEMBOURG	201,131	13	0.01
MALTA	36,990	13	0.04
MONACO	20,716	12	0.06
MONTENEGRO	8,893	5	0.06

COUNTRY	CAPITAL STOCK [MILLION USD]	AAL [MILLION USD]	AALR [%]
NETHERLANDS	3,410,955	238	0.01
NEW ZEALAND	679,705	23	0.00
NORTH MACEDONIA	32,996	26	0.08
NORWAY	1,933,679	10	0.00
POLAND	1,614,716	189	0.01
PORTUGAL	1,054,344	7	0.00
ROMANIA	555,697	256	0.05
SERBIA	57,317	33	0.06
SLOVAKIA	414,783	61	0.01
SLOVENIA	139,900	159	0.11
SPAIN	6,233,955	72	0.00
SWEDEN	1,747,501	5	0.00
SWITZERLAND	3,421,606	787	0.02
TURKEY	1,947,249	2,200	0.11
UNITED KINGDOM	7,806,797	892	0.01

6 Concluding Remarks

Testing of the European seismic risk model following the framework outlined in each Chapter presented herein will continue until the public release in October 2020. In particular, once the ESHM20 hazard model is available it will be used to repeat the system tests in Chapter 4 and to prepare the results for the acceptance tests described in Chapter 5.

Subsequently, a number of activities that are being developed in the European RISE project (www.rise-eu.org) will lead to improved testing of the model in the future. One such activity includes the development of a European ShakeMap system that will use the tectonic regionalization, ground motion logic tree and site amplification of the European hazard model, which can then be used in the tests outlined in Chapter 3. Another activity relates to the setting up of a European testing centre for hazard and risk models (similar to the 'CSEP center' in California, e.g. Schorlemmer et al., 2018). Once the ESRM20 is publicly released it will then be possible to design how the model (or its components) could be submitted for prospective testing.

7 References

- Akkar S, Bommer JJ (2010) "Empirical equations for the prediction of PGA, PGV, and spectral accelerations in Europe, the Mediterranean region, and the Middle East," *Seismological Research Letters*, 81 (2), 195–206.
- Bianchini M., Diotallevi P.P and Baker J.W. (2009) "Prediction of inelastic structural response using an average of spectral accelerations," *Proceedings of 10th International Conference on Structural Safety and Reliability (ICOSSAR09)*, Osaka, Japan
- Borzi B., Crowley H., Pinho R. (2008) "Simplified Pushover-Based Earthquake Loss Assessment (SP-BELA) Method for Masonry Buildings," *International Journal of Architectural Heritage*, <https://doi.org/10.1080/15583050701828178>
- Borzi B., Crowley H., Pinho R. (2008a) "The influence of infill panels on vulnerability curves for RC buildings," *Proceedings of 14th World Conference on Earthquake Engineering*, Beijing, China.
- Borzi B., Pinho R., Crowley H. (2007) "Simplified pushover-based vulnerability analysis for large-scale assessment of RC buildings," *Engineering Structures*, <https://doi.org/10.1016/j.engstruct.2007.05.021>
- Brzev S, Scawthorn C, Charleson AW, Allen L, Greene M, Jaiswal K., Silva V (2013) *GEM Building Taxonomy Version 2.0*, GEM Technical Report 2013-02 V1.0.0, 188 pp., GEM Foundation, Pavia, Italy.
- Crowley H, Despotaki V, Rodrigues D, Silva V, Toma-Danila D, Riga E, Karatzetsou A, Sousa L, Ozcebe S, Zugic Z, Gamba P (2020) "Exposure model for European Seismic Risk Assessment," *Earthquake Spectra*, *accepted for publication*.
- Dabbeek J, Silva V (2020) "Modeling the residential building stock in the Middle East for multi-hazard risk assessment," *Natural Hazards* 100:781–810. <https://doi.org/10.1007/s11069-019-03842-7>
- Del Gaudio C., De Martino G., Di Ludovico M., Verderame G.M. (2019) "Empirical fragility curves for masonry buildings after the 2009 L'Aquila, Italy, earthquake," *Bulletin of Earthquake Engineering*, 10.1007/s10518-019-00683-4
- Dolce M, Speranza E, Giordano F, Borzi B, Bocchi F, Conte C, Di Meo A, Faravelli M, Pascale V (2019) "Observed damage database of past Italian earthquakes: the Da.D.O WebGIS," *Bollettino di Geofisica Teorica ed Applicata*, 60(2), 141-164, DOI 10.4430/bgta0254
- EMDAT (2019) *International Disasters Database of the Centre for Research on the Epidemiology of Disasters*, available at <https://www.emdat.be/>
- ESYE - National Statistical Office of Greece, damage census. Athens, Greece 1999. <http://www.ceqid.org/CEQID/Study.aspx?p=32&ix=42&pid=38&prcid=40&ppid=620>
- Faenza L, Michelini A. (2010) "Regression analysis of MCS intensity and ground motion parameters in Italy and its application in ShakeMap," *Geophysical Journal International*, 180(3),1138–1152.
- Feranec J, Soukup T, Hazeu G, Jaffrain G (2016) *European Landscape Dynamics*. CRC Press, Boca Raton, FL : CRC Press, 2016.
- GAR (2015) *UNISDR 2015 Global Assessment Report*, available at www.preventionweb.net/english/hyogo/gar/2015
- GEM (2018) *Global Risk Map 2018.v1*, Available at www.globalquakemodel.org/gem
- Jaiswal K, Wald D (2013) "Estimating Economic Losses from Earthquakes Using an Empirical Approach," *Earthquake Spectra*, 29(1), 309-324.

- Jaiswal K, Wald D, Hearne M (2009) *Estimating casualties for large worldwide earthquakes using an empirical approach*, US Geological Survey Open-File Report 1136.
- Kappos AJ, Panagopoulos G, Penelis G (2008) "Development of a seismic damage and loss scenario for contemporary and historical buildings in Thessaloniki, Greece," *Soil Dynamics and Earthquake Engineering*, 28 (10–11), 836–850.
- Martins L, Silva V (2018) "A global database of vulnerability models for seismic risk assessment," *Proceedings of 16th European Conference on Earthquake Engineering*, 18-21 June 2018, Thessaloniki, Greece.
- Martins L, Silva V (2020) "Development of a Fragility and Vulnerability Model for Global Seismic Risk Analyses," *Bulletin of Earthquake Engineering, under review*.
- Milutinovic ZV, Trendafiloski GS (2003) RISK-UE project: an advanced approach to earthquake risk scenarios with applications to different European towns. WP04: vulnerability of current buildings, handbook.
- MunichRe (2019) *NatCatService*, available at <https://natcatservice.munichre.com/>
- Pagani M, Monelli D, Weatherill G, Danciu L, Crowley H, Silva V, Henshaw P, Butler L, Nastasi M, Panzeri L, Simionato M, Viganò D (2014) "OpenQuake Engine: An open hazard (and risk) software for the Global Earthquake Model," *Seismological Research Letters*, 85, 692-702.
- Penelis GG, Sarigiannis D, Stavrakakis E, Stylianidis KC (1988) "A statistical evaluation of damage to buildings in the Thessaloniki, Greece, earthquake of June, 20, 1978," *Proceedings of Ninth World Conference on Earthquake Engineering*, Tokyo-Kyoto, Japan, August 1988, Tokyo: Maruzen; 1988. p. VII:187–92.
- Pesaresi M, Ehrlich D, Florczyk AJ, Freire S, Julea A, Kemper T, Soille P, Syrris V (2015) GHS built-up grid, derived from Landsat, multitemporal (1975, 1990, 2000, 2014). In: Eur. Comm. Jt. Res. Cent. (JRC), [Dataset]. http://data.europa.eu/89h/jrc-ghsl-ghs_built_ldsmt_globe_r2015b. Accessed 24 Apr 2019
- Pitilakis K, Riga E, Karatzetzou A, Apostolaki S, Georgousaki A, Kiratzi A (2020) "Towards the development of a uniform seismic vulnerability and risk model in Europe. The cases of Athens and Thessaloniki, Greece," *Proceedings of 17th World Conference on Earthquake Engineering*, 13-18 September 2020, Sendai, Japan.
- Román MO, Wang Z, Sun Q, Kalb V, Miller SD, Molthan A, Schultz L, Bell J, et al (2018) "NASA's Black Marble night-time lights product suite," *Remote Sensing Environment* 210:113–143. <https://doi.org/10.1016/J.RSE.2018.03.017>
- Roumelioti Z, Kiratzi A, Theodulidis N, Kalogeras I, Stavrakakis G (2003) "Rupture directivity during the September 7, 1999 (Mw5.9) Athens (Greece) earthquake inferred from forward modelling of strong ground motion," *Pure and Applied Geophysics*, 160 (12), 2301–2318
- Roumelioti Z, Theodulidis N, Kiratzi A, (2007) "The 20 June 1978 Thessaloniki (northern Greece) earthquake revisited: slip distribution and forward modelling of geodetic and seismological observations" *Proceedings of 4th International Conference on Earthquake Geotechnical Engineering*. June 25-28, 2007. Paper No. 1594.
- Schorlemmer D, Werner MJ, Marzocchi W, Jordan TH, Ogata Y, Jackson DD, Mak S, Rhoades DA, Gerstenberger MC, Hirata N, Liukis M, Maechling PJ, Strader A, Taroni M, Wiemer S, Zechar JD, Zhuang J (2018) "The Collaboratory for the Study of Earthquake Predictability: Achievements and Priorities," *Seismological Research Letters*, 89(4), 1305–1313.

- SERA (2019a) *Deliverable D26.3 Methods for developing European commercial and industrial exposure models, and residential model update*, available at http://eu-risk.eucentre.it/wp-content/uploads/2019/08/SERA_D26.3_Exposure_Models_Non-res_Res.pdf
- SERA (2019b) (Romão et al. 2019) *Deliverable D26.5 European physical vulnerability models*, available at http://eu-risk.eucentre.it/wp-content/uploads/2019/08/SERA_D26.5_Physical_Vulnerability.pdf
- SERA (2019c) *Deliverable D26.4: Methods for Estimating Site Effects in Risk Assessments*, available at http://eu-risk.eucentre.it/wp-content/uploads/2019/08/SERA_D26.4_Site_Amplification_Risk_Assessment.pdf.
- Silva V, Amo-Oduro D, Caldero A, Costa C, Dabbeek J, Despotaki V, Martins L, Pagani M, Rao A, Simionato M, Viganò D, Yepes-Estrada C, Acevedo A, Crowley H, Horspool N, Jaiswal K, Journeay M, Pittore M (2020) “Development of a Global Seismic Risk Model,” *Earthquake Spectra*, doi: 10.1177/8755293019899953
- Silva V, Crowley H, Pagani M, Monelli D, and Pinho R (2014) “Development of the OpenQuake engine, the Global Earthquake Model’s open-source software for seismic risk assessment,” *Natural Hazards*, doi:10.1007/s11069-013-0618-x.
- Silva V, Horspool N (2019) “Combining USGS ShakeMaps and the OpenQuake-engine for damage and loss assessment,” *Earthquake Engineering and Structural Dynamics*, doi: 10.1002/eqe.3154.
- Villar-Vega M, Silva V (2017) “Assessment of earthquake damage considering the characteristics of past events in South America,” *Soil Dynamics and Earthquake Engineering*, 99, 86-96.
- Wald DJ, Allen TI (2007) “Topographic slope as a proxy for seismic site conditions and amplification,” *Bulletin of the Seismological Society of America*, 97 (5), 1379-1395.
- Woessner J, Danciu L, Giardini D, Crowley H, Cotton F, Grünthal G, Valensise G, Arvidsson R, Basili R, Demircioglu MB, Hiemer S, Meletti C, Musson RMW, Rovida AN, Sesetyan K, Stucchi M, The SHARE Consortium (2015) “The 2013 European Seismic Hazard Model: Key Components and Results,” *Bulletin of Earthquake Engineering*, 13 (12), 3553–3596.

Contact

Project lead	ETH Zürich
Project coordinator	Prof. Dr. Domenico Giardini
Project manager	Dr. Kauzar Saleh
Project office	ETH Department of Earth Sciences Sonneggstrasse 5, NO H62, CH-8092 Zürich sera_office@erdw.ethz.ch +41 44 632 9690
Project website	www.sera-eu.org

Liability claim

The European Commission is not responsible for any use that may be made of the information contained in this document. Also, responsibility for the information and views expressed in this document lies entirely with the author(s).